EXPERIMENTAL STUDY OF WAVE SLAMMING OF SANDWICH COMPOSITES PANELS

By

Samuel Charca Mamani

A thesis submitted in partial fulfillment of the requirements for the degree of

DOCTOR OF PHILOSOPHY
in
CIVIL ENGINEERING
(Structures)

UNIVERSITY OF PUERTO RICO
MAYAGÜEZ CAMPUS

2009

Approved by:

Basir Shafiq, PhD President, Graduate Committee	Date
Luis A. Godoy, PhD Member, Graduate Committee	Date
Ricardo R. López, PhD Member, Graduate Committee	Date
Luis E. Suárez, PhD Member, Graduate Committee	Date
Frederick Just, PhD Member, Graduate Committee	Date
Ernesto Otero, PhD Representative of Graduate Studies	Date
Ismael Pagán Trinidad, Prof. Chairperson of the Department	Date

ABSTRACT

Slamming of ship hull structures was simulated using sandwich composite panels that were repeatedly slammed on to a body of calm water with the main objective of understanding the damage accumulation mechanism and corresponding lifetime. Literature is abundant on ship hull slamming; however, it is limited to single slamming; while damage accumulation and progression under repeated slamming is largely absent. Therefore, an extensive experimental program was carried out to understand damage accumulation and failure in sandwich composites under repeated slamming as a function of deadrise angle and slamming energy. The two model material systems used consisted of polyester foam filled honeycomb sandwich composites and polyurethane foam core sandwich composites. Honeycomb core sandwich composites indicted a significant damage accumulation as a function of increasing slamming energy. Similarly, foam core sandwich composites revealed a gradual but substantial damage accumulation as a function of increasing slamming energy or decreasing deadrise angle. The modes of failure corresponded primarily to local facesheet yielding with evidence of core crushing for the honeycomb core sandwich composites. While, the modes of failure indicated mainly interface tearing, core shear and facesheet buckling in the case of foam core sandwich composites. Interestingly, the peak pressures and strains were observed to occur near the keel while the maximum damage was obtained near the chine at deadrise angles between 15^{o} and 20^{o}; as ship hull design is primarily based on peak pressures, this result is quite significant.

RESUMEN

El impacto de la estructura del casco sobre la superficie de agua fue simulado usando placas de compuestos sándwich con el objeto de estudiar el comportamiento de estos bajo impactos repetitivos. Existe abundante literatura con respecto a impactos sencillos sin embargo para impactos repetitivos no existe investigaciones previas para determinar los mecanismos y la acumulación de daño. Esta investigación esta enfocada en desarrollar un programa de experimentaciones, que nos permita entender el daño acumulado y las fallas que se producen bajo impactos repetitivos como función de la energía y ángulo de impacto. Dos materiales se usaron, compuestos sándwich con núcleo panal llenado con espuma de poliéster y compuestos sándwich como núcleo espuma de poliuretano. Los compuestos de panal sufrieron un significativo daño como función del incremento de la energía de impacto. De la misma manera los compuestos de poliuretano sufrieron un daño sustancial como función del incremento de la energía y ángulo de impacto. Los modos de falla principales fueron fluencia local con un aplastamiento de la zona de factura para los compuestos de panel. Mientras falla por interfase, cortante del núcleo y pandeo local fueron para los compuestos de poliuretano. Las presiones y deformación unitarias máximas se localizaron en la zona de la quilla, no obstante los danos máximos ocurren en la zona opuesta, esto se observo para ángulos de impacto de 15^o y 20^o, en el diseño del casco de los barcos se usan las presiones máximas por consiguiente este resultado es muy significativo como propósito de análisis.

.

To my parents Melquíades and Cecilia; my sister and brothers: Lucre, Daniel, Marcial, Albino, and Jaime; my nieces and nephews: Nelly, Evelin, Rubí (Ceci), Alexander, and Marcel; and finally to Gianny; for their immensurable support and love

ACKNOWLEDGEMENTS

During the development of my graduate studies in the University of Puerto Rico several persons directly or indirectly supported my research for which I am grateful. This section is dedicated to recognize their support.

First of all, thanks to my advisor, Dr. Basir Shafiq for his encouragement, support and guidance in the development of this thesis; I consider myself fortunate to be his student. I would like to also thank Dr. Frederick Just and Dr. David Serrano who helped me grow as an investigator. Also I wish to thank the Dr. Yapa Rajapakse, the ONR program manager for funding this research (ONR grant #N000140611043). I also wish to express my thinks to the General Engineering Department of University of Puerto Rico-Mayagüez for offering me assistantship during the entire Ph.D. program.

My special thanks to my friends Omar López, Sergio González, Evaristo Figueroa, and Alexander Peralta for their dedication to help me carry out the fabrication of slamming machine, slamming samples and general experimental work.

Finally I must thank the Laboratory Group Guinevere Just and Pedro Velasquez for making the laboratory a comfortable place to work.

Table Of Contents

Table List

Tables **Page**

Figure List

Figures **Page**

List of Symbols and Abbreviation

AE	Acoustic emission
ASTM	American society of testing and materials
b	Beam wide
C	Shear modulus exponential coefficient
CT	Curing time
c	Wetted half beam
cps	Centipoises
d	Distance from dextral axis to the half of facesheet
dB	Decibels
d_f	Damage under fatigue
d_s	Damage under slamming
E	Modulus of elasticity
E_c	Core modulus of elasticity
E_f	Facesheet modulus of elasticity
E_n	Slamming energy
E_{ult}	Slamming energy to cause permanent failure
FCG	Fatigue crack growth
FEA	Finite element analysis
I	Beam moment of inertia
l	Beam length
M	Inertia (mass) of the slamming assembly
N	Number of cycles to cause failure
NDT	Non destructive testing
p	Pressure imposed in the wedge
p_a	Added mass pressure
S_s	Slope of the slamming lifetime
t_c	Core thickness

t_f	Facesheet thickness
V	Water entry velocity
VARTM	Vacuum Assisted Resin Transfer Molding
V_s	Wave propagation velocity
W	Wedge weight
y	Distance from neutral axis to facesheet
z	Vertical coordinate on the wedge
β	Deadrise angle
ε	Strain
ε_{utl}	Threshold strain causing catastrophic failure
κ	Adjusted parameter for safe operational equation
η	Adjusted parameter for hydroelasticity function
ρ	Water density
φ	Velocity potential
σ	Material strength
σ_{ult}	Ultimate strength
μ_H	Hydroelasticity function
w	Beam deflection

1 INTRODUCTION

1.1 Justification

High speed lightweight marine craft operating in rough seas undergo a complex loading environment principally as a result of repeated slamming of the ship hull onto the ocean waves. The existing theories, being limited to single slamming fail to account for the long term failure occurrences and modes of failure that are critical in establishing a viable life prediction methodology. Clearly, damage/failure information is indispensable in making a meaningful service life assessment and to avoid detrimental consequences. However, discerning modes of failure in sandwich composites subjected to repetitive slamming load remains a significant challenging due mainly to lack of viable in-situ damage detection instrumentation. As a result, post slamming techniques are generally employed to ascertain the state of damage in the material. In this thesis, post slamming static and fatigue testing is adopted in order to determine cumulative damage and modes of failure in sandwich composites subject to single and repeated slamming scenario. The resulting damage information is subsequently used to develop a remaining lifetime model applicable to sandwich composite materials subject to repeated slamming.

1.2 Objectives

The main objective of this thesis is to obtain meaningful damage information that can advance the understanding of sandwich composite failure characteristics subjected to repeated low amplitude slamming. The specific tasks are:

a) Quantify the effect of slamming on the state of damage in foam core sandwich composites as a function of drop height (energy of impact, E_n), deadrise angle (β).
b) Develop and implement a methodology to discern modes of failure and accumulated damage associated with the simulated wave slamming on sandwich composites.

c) Develop a semi-empirical model to relate the effect of repeated slamming on the remaining strength and fatigue life of the material.

1.3 Significance

Material characterization under repeated wave slamming is crucial for accurate design, maintenance and remaining lifetime assessment of sandwich composites. The work is unique as the literature is non-existent on the repeated slamming of sandwich composites and scarce on the modes of failure and damage under slamming.

2 LITERATURE REVIEW

Impulse loads with high pressure peaks occur during impact between a body and water, which is often called slamming that takes place when a ship bottom (bow) hits the water at a high velocity. Observations of slamming phenomena on actual ships indicate a violent and repetitive impact of ship bottom onto the water with acceleration rise time and duration in the order of milliseconds this makes the test design, instrumentation and in-situ data collection a difficult task. The hydrodynamics pressure causing this acceleration response of almost 10g constitutes a peak propagation that is difficult to predict [1-5]. Therefore, the hulls must be light enough and yet stiff enough to withstand these loads. A sandwich composite is a special form of laminated shell structure that consists of distinct three layers that are bonded together to form an efficient load carrying assembly. The high stiffness, light weight and energy absorption gives the sandwich composites an advantage over conventional materials used in the marine industry [6]. As most modern day marine craft operate at high speeds subjected to repeated wave slamming loads, the prediction of safe operational life gains paramount importance especially in newly developed sandwich composite ship hull structures [7, 8].

Abundant literature is available on the wave slamming of ship hulls on water, however most of the work is limited to one-strike impact. Wagner and Von Karman [9, 10] are considered the pioneers in the field of solid to fluid impact and have proposed models to predict the pressure distribution along the wedge shaped model samples. Their analytical work has essentially formed the basis of much of ship hull design and analysis. Wagner [9] simulated a wedge setup as a boundary value problem to acquire results corresponding to slamming pressure distribution that depend on structural form and time dependent water entry velocity. Wagner's model may be represented in the following form

$$p - p_a = \rho V \frac{c}{\left(c^2 - x^2\right)^{1/2}} \frac{dc}{dt} + \rho \frac{dV}{dt}\left(c^2 - x^2\right)^{1/2} \qquad (1)$$

Where p denotes the slamming pressure and p_a refers to the added mass pressure that incorporates the hydrodynamic forces ($p=p_a$ on the free surface). The transversal coordinate 'x' is measured from the keel of the wedge, c is the wetted half beam expressed as $c(t) = \pi Vt / 2\tan\beta$, where β is the deadrise angle. dc/dt corresponds to rate of change of wetted surface and V emerges from the "velocity potential" as $\frac{\partial \varphi}{\partial z} = -V \;\; , \varphi = -V\left(c^2 - x^2\right)^{1/2}$. According to Eq. 1, the maximum pressure is limited to $P_{\max} = \frac{1}{2}\rho\left(\frac{dc}{dt}\right)^2$ when the velocity is constant and $|x| \rightarrow c(t)$. Von Karman [10] also analyzing a symmetric wedge entering a calm body of water used conservation of momentum to describe the average pressure imposed on the wedges in the following form,

$$p = \frac{\rho V^2}{2} \frac{\pi \cot\beta}{\left(1 + \frac{\gamma \pi x^2}{2W}\right)^3} \qquad (2)$$

where p is the maximum pressure taking place at the moment of first contact and W is the weight and is the ρ fluid density. Eq. 2 suggests that the maximum pressure takes place at x=0. One of the main differences between Wagner [9] and Von Karman [10] model is that Von Karman neglects the local uprise of water upon impact that leaves the wetted surface to be smaller.

Since then, many other researchers have made significant analytical and experimental contributions to the study of wave slamming of ships. Some of the earliest reported wave impact studies were motivated by landing sea planes and planning crafts; a substantial review of these early contributions can be found elsewhere [4, 11]. Computational techniques, such as finite and boundary element analysis, have been widely used to study pressure profile along with various other aspects of wave slamming by combining hydrostatic and hydrodynamic analysis. The problem of fluid structure interaction is generally made difficult by continuously moving boundaries between the hull and the water surface and coupling of hydroelasticity and structural response. The problem can be simplified by assuming inviscid, incompressible and irrotational potential flow, as well as by limiting the degrees of freedom of motion, reducing the general three dimensional problem to a series of two dimensional sections and most importantly by assuming that the loads can be applied quasi-statically, i.e., no hydroelastic interaction occurs and the hydrodynamic loads and structural response can be treated separately [1-3, 12-14]. This leads to great simplifications in the solution of Navier Stokes and continuity equations and significantly reduces the computational time.

Hydroelasticity can be defined as the interaction of the fluid and the structure, i.e., during the impact, the water pressure acts on the structure and the structure deforms and simultaneously as a consequence of structural deformation, the pressure is induced on the water domain. With the current state of knowledge, the assumption of quasi-static loads is almost required, however, questions linger about its validity [4, 15]. Generally, if the body is assumed rigid, the quasi-static theory may apply and the effect of hydroelasticity may be ignored, however, doing so risks overestimating the pressure response on the structures as no structure is perfectly rigid [12, 13, 16]. In reality it is impossible to formulate a uniform design pressure which is equivalent to the real hydrodynamic loads, especially in sandwich composite structures where the margin of failure is so different in various constituents of the material. Bereznitski [13] studied the hydroelasticity as a function of deadrise angle, material stiffness and the air entrapment using explicit Finite Element Analysis (FEA) and found that the ratio between the duration of the impact and the first period of the natural frequency is the key parameter that determines whether the effects of hydroelasticity are significant enough to be considered in the analysis; if the ratio is greater than 2.0, the effect of hydroelasticity may be ignored. Faltinsen et.al. [17] studied hydroelasticity using hydroelastic orthotropic plate theory and illustrated the importance of hydroelasticity by presenting non-dimensional structural response in relation to loading period and wet natural period of the structure. Their theoretical work substantiated by experimental verification suggested that during bow flare, the effects of hydroelasticity are not locally significant, but global influences are manifested in the form of whipping (transient hydroelastic response). However, when the local loads become very high during slamming, effects of hydroelasticity could become significant. Stenius [15] following a similar analysis, concluded that if the ratio of loading period and natural period is greater than 5, then the hydroelastic effects may be ignored. As a general guideline, if the first natural period of vibration is distinctly smaller than the shortest loading period, then the structural deformations are small and the structure can be assumed rigid and treated with the quasi-static loading assumption [8]. Using quasi-static assumption, with pressure taken from Wagner's theory, Eq. 1 [9] and elementary beam theory, the panel deflections and strains can be written as [15],

$$w = \mu \frac{\rho \pi^2 V^2 l^4}{1536 EI \tan \beta} \qquad or \qquad \varepsilon = \frac{\sigma}{E} = \frac{My/I}{E} = \frac{\frac{Pl^2 y}{8}/I}{E} = \frac{\rho \pi^2 byV^2 l^2}{32 EI \tan \beta} \qquad (3)$$

On the other hand, if the quasi-static theory is not applicable, the problem has to be treated as a hydroelastic problem, which means solving coupled non-linear differential equations.

Some of the other issues related to slamming phenomena deal with incompressibility, discrete pressure information, effect of constant velocity, strains, vibrations, and scatter in the data. It appears conclusive that the slamming pressures do not appreciably depend on the compressibility of the fluid [14, 18]. Impact pressures are characterized by large gradients and rapid development and propagation across the hull surface, and measurements with transducers in discrete positions do not generally give any direct information about the pressure magnitudes between transducers. In order to address this problem, Rosen [3] developed an interpolative numerical scheme that takes a few discrete pressure data points and generates the profile for impact pressure distribution. Faltinsen [14] concluded that the impact pressure can be extremely high during the initial phase of impact such that the maximum deflection and stresses that are linearly proportional to the impact velocity occur during the first half oscillation period and are the most important results from a practical point of view [8, 14]. Controlled velocity experiments have recently been conducted on ship hull materials including sandwich composites [6, 15, 19-21]. The effect of constancy of velocity during impact appears to have little to no significance in the peak pressures obtained. Changes in velocity do influence the hydroelastic behavior of the material, however, not to a great extent as the critical pressure readings come during initial contact only, while the pressure during the subsequent submergence of the body into water tends to be substantially lower [1, 14, 22]. Reduction of velocity just after the impact has been reported to be inversely proportional to the drop height [23]. Some researchers have found large scatter in the measured pressure distribution data under drop tests and suggest that the impact problem should not be treated in a deterministic manner even when the environment is deterministic, especially when the peak pressures are involved [14, 24].

Even though the phenomenon of wave slamming has been under investigation for nearly a century, fully instrumented experimental verification did not surface until a few decades ago. Testing of complete hulls in the marine environment have been performed, however, it remains a cost prohibitive proposition [1, 4, 21, 23, 24]. Furthermore, the facilities are not readily available to conduct a full scale testing, therefore, much of the laboratory work on testing for wave slamming has been limited to free or controlled dropping of flat panels mounted on v-shaped rigid supports from predetermined heights onto a body of calm water [2, 11, 15, 20, 21, 23-25]. The samples are generally instrumented with piezoelectric pressure sensors, strain gauges and accelerometers and testing is performed as a function of deadrise angle which has significant influence on the pressure distribution. Slamming pressure increases as the deadrise angle decreases (i.e. increased bow flare).

Data collection and analysis is also a major issue in slamming tests. Identification of signal peaks, filtration of noise, frequency of data collection and sheer enormity and stochastic nature of data becomes a significant challenge to deal with [1, 24, 26]. In full scale or model drop tests measurements with pressure transducers, strain gauges, accelerometers, etc. gives only discrete information. In order to get complete information, either very large number of transducers is needed or complex interpolation of signal analysis is required, perhaps using some form of neural network analysis. Furthermore, discrete strain or pressure information can not be used in a meaningful way to discern failure events in sandwich composites in real time, which is a major limitation of the current instrumentation.

Wave slamming in reality induces repeated impulsive pressure each lasting a very short duration (in millisecond) at a very high speed that results into complex failure modes, which is neither clear analytically or experimentally in the literature at this time. Sandwich structures are composed of widely different constituents that display peculiar failure modes as a consequence of complex in-service cyclic slamming impact loads. These loads over time can cause core crushing, shear failure in the core, facesheet-core debonding and compressive or tensile failure of the laminates that can lead to global reduction in the load carrying capability of the hull and compromise the seaworthiness of the ship. However, defining failure and discerning the failure events in sandwich composites under repeated slamming scenario is not a trivial task. Under slamming impact, the facesheets generally remain intact and free of any visible damage for most of the sandwich composite lifetime, therefore, any surface anomalies are hard to relate to failure events in the core and the interface where failure is likely to initiate and propagate. Clearly, without any damage/failure information, it is impossible to develop a meaningful reliability and life prediction methodology.

Quasi-static and fatigue lifetime assessment is not only a crucial intermediate step between specimen design and service, it can also be used as a useful post slamming tool to assess cumulative damage in the material. However, unlike homogeneous materials, failure characterization is rendered quite complex in sandwich composites due to the presence of various constituents of differing elastic properties, presence of multiple cracks, and general lack of viable instrumentation for in-situ characterization [26-28]. It is generally desired that the core failure precedes facesheet failure in order to prevent water ingress and catastrophic failure. Therefore, failure in sandwich composites under fatigue loading generally degrades the softer core or the interface between the core and an order of magnitude stiffer facesheets which is difficult to detect by optical means [26, 29]. Additional difficulties arise from large scatter in the lifetime data that necessitates stochastic analysis [30, 31]. Fatigue of sandwich composites have been known to be sensitive to effect of notches, frequency changes, the loading ratio and environment to name a few; a substantial review of the fatigue of sandwich composites research can be found elsewhere [32].

In contrast to many conventional non-destructive evaluation (NDE) techniques, acoustic emission (AE) technique permits continuous damage inspection, classification and identification of modes of failure in various constituents of the composite in real time, which is critical for taking preventive measures [33, 34]. In spite of widespread use of AE technique in various engineering applications [33-41]; literature on the AE application in fatigue crack growth (FCG) monitoring in sandwich composites is scarce [26-28, 42]. AE technique, though useful, requires significant preliminary analysis and calibration for each system of material involved, geometry and type of loading to distinguish among various types of damage and failure mechanisms. Threshold frequencies that are material dependent need to be accurately set to filter out spurious noises without interfering with the useful data [28, 30, 33, 36]. Furthermore, shear enormity of AE data under fatigue testing makes the analysis demanding and time consuming. Nevertheless, the payoff in terms of being able to discern failure events that can easily go unnoticed with other damage detection techniques far outweighs the drawbacks.

3 EXPERIMENTAL PROGRAM/SETUP

3.1 Experimental Approach

The flow chart shown in Fig. 1 outlines the experimental approach

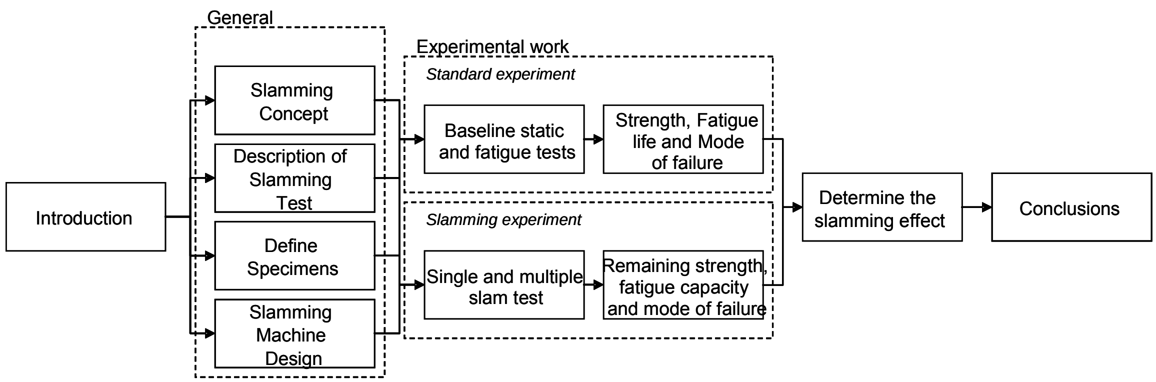

Figure 1: Research flow chart to investigate the sandwich composite panels under slamming

Substantial effort has been expended to explore ways to detect progressive failure events in sandwich composite panels subjected to repeated slamming impact. Strain gauges yield only discrete information and furthermore, do not discern failure in various constituent of the sandwich composite. Similarly, discrete information obtained from the pressure sensors can not be extrapolated to discern modes of failure. Acoustic emission sensors that have been implemented in static and fatigue testing in sandwich composites were thoroughly checked for their viability in detecting failure events under slamming but with little success due to excessive and incompatible acoustic frequencies that obscured the actual failure events [42]. In addition, AE sensors also failed as they function best when damage is localized while damage under slamming is wide spread in various constituents of the sandwich composite, thus rendering AE techniques inept. As a result, with the available instrumentation, it seems unlikely to assess the extent of damage in real time in specimens subject to cyclic slamming impact. This poses a significant practical inconvenience, as unless there is catastrophic failure, it is impossible to know when to stop the test. Therefore, failure in sandwich composites has to be defined and a methodology has to be developed that would permit quantification of this failure.

Faced with this enormous challenge, an indirect technique is being proposed in this thesis in order to extract accumulated damage information in post slamming specimens in terms of remaining strength and fatigue lifetime. The proposed technique can also help in localizing the extent of damage suffered during the slamming process. The steps involved are outlined in the following and detailed in the flow chart given in Fig. 2.

a) Establish baseline stress-strain ($\sigma-\varepsilon$) curve from static tests and obtain the ultimate static strength (σ_{ult}). These tests are performed on a servo hydraulic machine.
b) Establish fatigue life from tests performed at a predetermined percentage of ultimate static stress level ($X\%\sigma_{ult}$). These tests are performed on a servo hydraulic machine.
c) Obtain the ultimate energy to failure (E_{ult}) by subjecting the specimens to one-slam impact performed at various energy (height) levels.
d) Based on the ultimate impact energy to failure, repeated slamming impact tests are conducted.
    i. Material #1: at fixed percentage of ultimate energy ($Y\%E_{ult}$) and for various predetermined number of cycles (N_s) as illustrated in Table 1a.
    ii. Material #2: complete a slamming lifetime curve as a function of dead rise angle, furthermore perform a test at certain $\%E_{ult}$ up to 50% of the average slamming lifetime (refers to Table 1b).
e) Finally, each of the material systems (i) and (ii) tested under repeated slamming is sectioned into three zones, namely, a high impact pressure zone – the lower part of the specimens and a low impact pressure zone – the upper part of the specimen. The samples obtained are instrumented with AE sensors and tested under static and fatigue loading in the servo hydraulic machine to obtain remaining strength from the quasi-static tests (i and ii) and remaining fatigue lifetime obtained from load controlled fatigue tests conducted at the same load level ($X\%\sigma_{ult}$) as in step b (ii). From the remaining strength

and fatigue life, cumulative damage and modes of failure information are deduced that are used to establish the life prediction model.

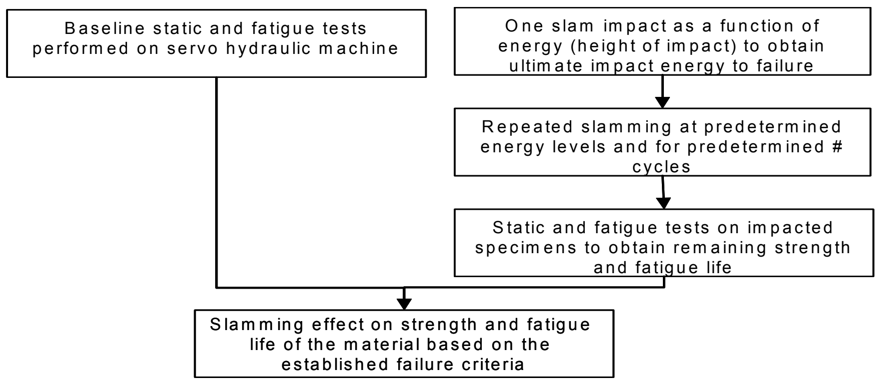

Figure 2: Test procedure to study the remaining strength and fatigue life.

Table 1a: Test program for polyester foam filled honeycomb core sandwich composite

Type of Test		**Number of specimens**
Static and Fatigue Test - Specimen Dimensions 12x2.5x1/8 in^3		
Static	Obtain $\sigma-\varepsilon$ curve and σ_{ult}	4
Slamming Test – Specimen Dimensions 12x2.5x1/8 in^3		
Single Slam (at various heights to obtain E_{ult})	$E_1, E_2, \ldots, E_n$	Minimum 3 at each energy level
Cyclic Slamming (conducted at % of E_{ult})	50 cycles @E_i	3
	50 cycles @E_{ii}	3
	50 cycles @E_{iii}	3
Remaining Strength – Specimen Dimensions 12x2.5x1/8 in^3		
Static flexure	50 cycles @E_i	9 (3 at each zone)
	50 cycles @E_{ii}	9 (3 at each zone)
	50 cycles @E_{iii}	9 (3 at each zone)

Table 1b: Test program for polyurethane foam core sandwich composites

Type of Test		Number of specimens
Static and Fatigue Test - Specimen Dimensions 12x2.5x1/2 in^3		
Static	Obtain $\sigma-\varepsilon$ curve and σ_{ult}	5
Fatigue	X% σ_{ult}	5
Slamming Test – Specimen Dimensions 12x9x1/2 in^3		
Single Slam (at various E_n to obtain E_{ult}) to different β	E_1	4
	E_2	4
	E_n	4
Repeated Slamming (conducted at Y% of E_{ult}) to different β	$Y_1\%E_u$	6
	$Y_2\%E_u$	6
	$Y_n\%E_u$	6
Partial Repeated Slamming (for angle)	$50\%N_f$	12
Remaining Static Strength and Fatigue Lifetime – Specimen Dimensions 12x2.5x1/2 in^3		
Static (for angle)	50%Nf	6
Fatigue (conducted at X% of P_{ult}, for angle)	50%Nf	6

3.1.1 Materials, Static and Fatigue Test

Two types of sandwich composites were used in the experiment: **Material #1, polyester foam filled craft paper honeycomb with $[0/90]_1$ carbon fiber facesheets**, 0.5% of special nano-clay was used in the epoxy resin in order to enhance the interface properties detailed in Fig. 3, **Material #2, polyurethane foam core sandwich composites** were made of 161 g single carbon fiber $0^o/90^o$ 3K one plain weave facesheet of 0.5 mm thickness and a 12.5 mm thick polyurethane foam core of 96.11kg/m^3 density. The resin was a 635cps thin epoxy. Vacuum Assisted Resin Transfer Molding (VARTM) technique was employed to fabricate the specimens [26, 29, 43]. The mechanical properties for both of them are shown in Tables 2a,b.

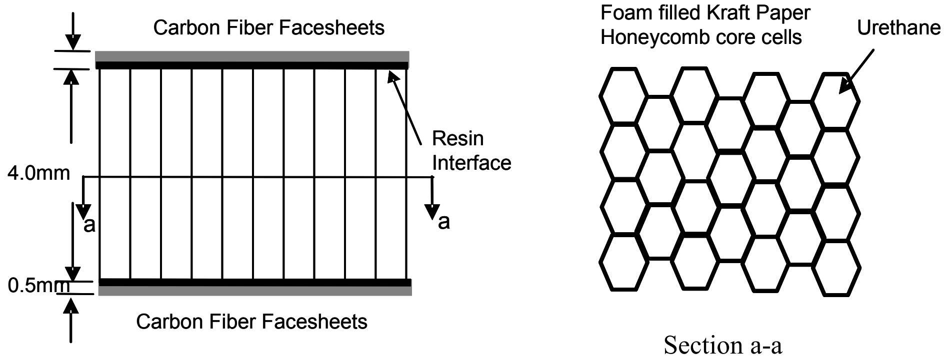

Figure 3: Polyester foam filled honeycomb core sandwich composite; dimensions, lateral and top view of the honeycomb

Table 2a: Mechanical properties of polyester foam filled honeycomb core sandwich composites

Property	**Face sheet**	**Foam core**
Mass Density (kg/m^3)	1117	89
Longitudinal modulus of elasticity (MPa)	$40x10^3$	7.45
Transversal modulus of elasticity (MPa)	$40x10^3$	7.45
Longitudinal shear modulus of elasticity (MPa)	$10x10^3$	0.998
Transversal shear modulus of elasticity (kPa)	$10x10^3$	0.998
Poisson's Ratio	0.32	0.3

Table 2b: Mechanical properties of polyurethane foam core sandwich composite

Property	**Face sheet**	**Foam core**
Mass Density (kg/m^3)	1117	96
Longitudinal modulus of elasticity (MPa)	$40x10^3$	21.507
Transversal modulus of elasticity (MPa)	$40x10^3$	21.507
Longitudinal shear modulus of elasticity (MPa)	$10x10^3$	8.994
Transversal shear modulus of elasticity (kPa)	$10x10^3$	8.626
Poisson's Ratio	0.35	0.3

Flexural testing was performed on a servo-hydraulic testing machine attached to a data acquisition system, an eight channel AE setup, and a digital traveling microscope. The test setup along with the details of the specimen geometry is shown in Figs. 4 and 5. Flat metal plates with rubber pads were used to minimize indentation damage to the specimen under loading. Flexural quasi-static strength was performed at 100N/min and the fatigue tests were performed between stress levels of 60 and 90% of the ultimate static load at a load ratio of 0.1 and a frequency of 1Hz.

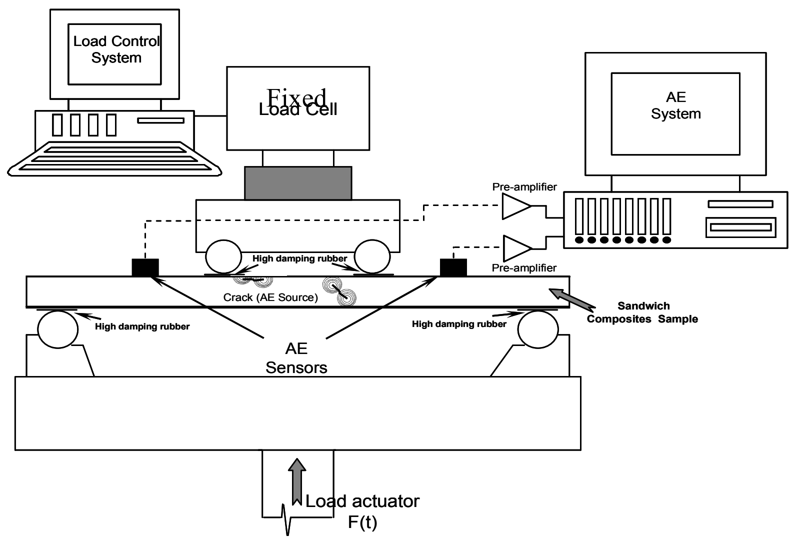

Figure 4: Static and fatigue experimental test setup monitored by AE technique

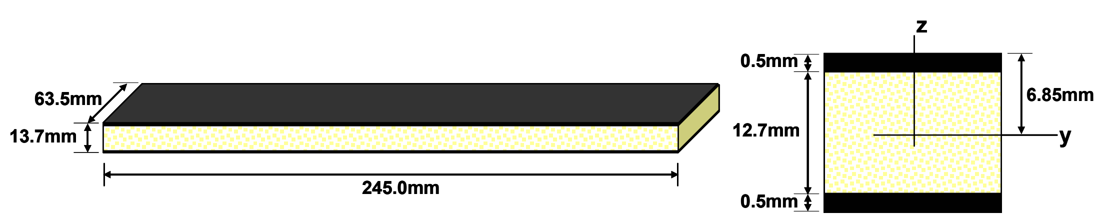

Figure 5: Sandwich composite beam dimensions

Cutoff in composite materials is generally set in the range of several million cycles to obtain the endurance limit, especially in materials where a large scatter in the data is observed. However, motivated mainly by time constraints, tests were terminated at an arbitrary number of 500,000 cycles. The cutoff was based on the criteria that disallowed any failure activity in the facesheet or in the interface between the facesheet and the core, while permitting less than 20% of the average the AE events activity (in the foam) as compared to the failed specimens. The AE activity in the foam core ensues almost instantaneously as the test starts and accounts for initial accommodation, release of residual stresses and friction, etc. However, a cumulative 20% activity in the foam core is far below what precedes failure in the specimens, and thus was accepted within the 500,000 cycle cutoff.

Fig. 4 shows the sketch of AE system with two Pico-sensors used in a linear array on the specimen surface at an adequate distance from each other. The system is calibrated using ASTM E976 standard [42]. Thresholds are established to filter and minimize extraneous background and frictional noise; in addition high damping rubber is used around the loading pins to minimize contact noise and damage induced by indentation.

In order to locate the source and extent of damage, acoustic wave speeds were calculated according to ASTM E976 standard [44]. For the sandwich composite used, average values of wave speeds were found to be 3170 m/s (with 44 m/s standard deviation) and 1043 m/s (with 61 m/s standard deviation), in the longitudinal and through the thickness directions, respectively. Wave speeds did not agree well with published results (of other sandwich composite systems) as AE parameters highly depend on the material type and geometry [40, 41, 45, 46].

3.1.2 Slamming Machine Design and Fabrication

The free drop slamming system was designed and fabricated in-house. Both one-strike and repeated slamming can be performed from various heights corresponding to the desired energy level. The specimen sizes and deadrise angle of the symmetric wedge can also be varied. Various boundary conditions can be imposed, however, simply supported end supports is used in this set of testing. A gear system attached to a continuously rotating motor engages and disengages at preset time intervals in order to rise and release the wedge shaped specimen assembly from pre-determined heights. The interval between each slamming event is set at 30 seconds (0.033 Hz) to allow the water to regain its initially calm state. A 1.80-m diameter and 1.25-m depth water tank is used to slam the symmetric wedge specimen holder. Baffles are used around the tank to minimize the wave reflection. The details of wave slamming apparatus and setup are illustrated in Fig. 5.

a)

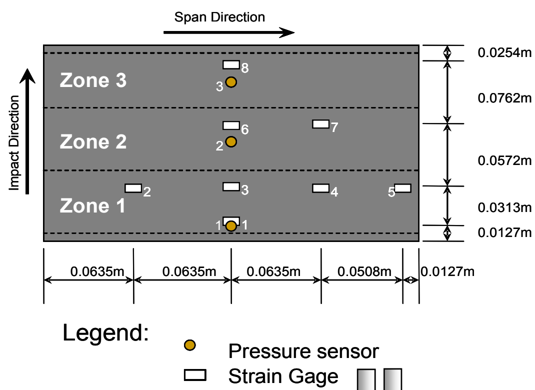

b)

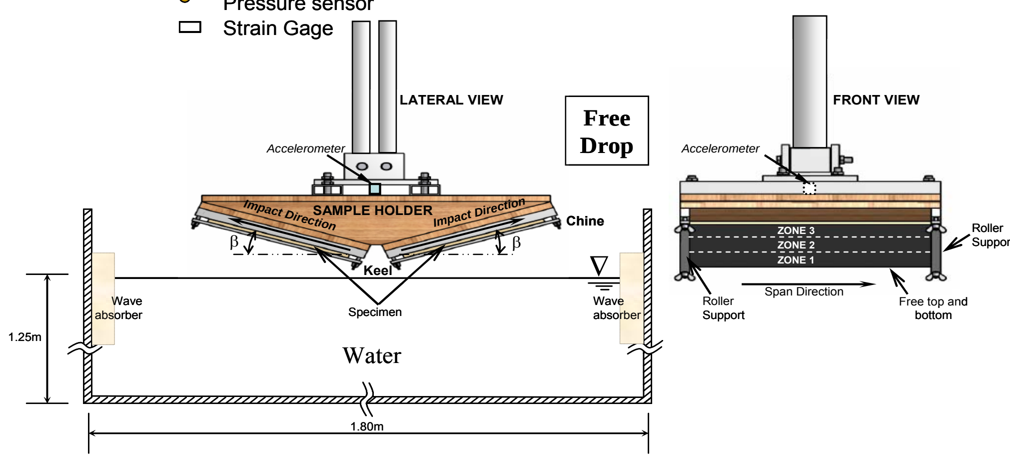

Figure 5: a) Slamming sandwich composite panel dimensions, pressure ands train gage sensors setting, and b) experimental setup for single and repeated slamming, where β is the deadrise angle

The slamming specimens are instrumented with piezo-electric pressure, strain, transducers and accelerometer. The Pressure sensors are installed on the impact faces in the maximum pressure zone; whereas the strain gages are mounted on the back faces with same configuration, see Fig. 5. The accelerometer is mounted on the inside of the sample holder.

4 FATIGUE LIFETIME OF FOAM CORE SANDWICH COMPOSITES [57]

This chapter presents the results obtained from mechanical characterization of polyurethane foam core sandwich composite

4.1 Preliminary Results

Although VARTM process is known for its consistency, post fabrication microscopic analysis indicated that penetration of resin into the foam ranged randomly from 200μm-500μm, as illustrated in Fig 6a and approximately is two to three times of closed cell diameter (Fig. 6b) that may exert some influence in the fatigue lifetime. Curing time and resin shrinkage was also carefully analyzed to evaluate the presence and extent of residual stresses. Plots of curing time vs. strength evolution along with associated cumulative AE events are presented in Fig. 7a, b. The modes of failure were observed to change from ductile crushing and indentation of the facesheets to mostly core crushing as a function of increasing curing time as detailed in Fig 8. The average curing time was recorded at 500 hours yielding the flexural capacity of 840N when tested at a rate of loading of 100N/m. This flexural capacity was used as the basis for the design of fatigue tests.

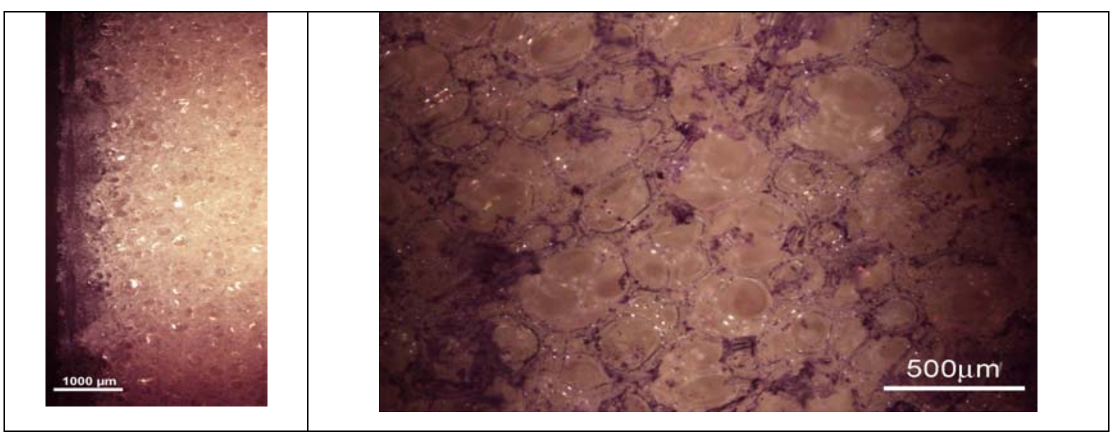

Figure 6: a) Resin distribution into the foam, and b) polyurethane foam micrograph, the diameter of the close cell foam is ~179.48μm

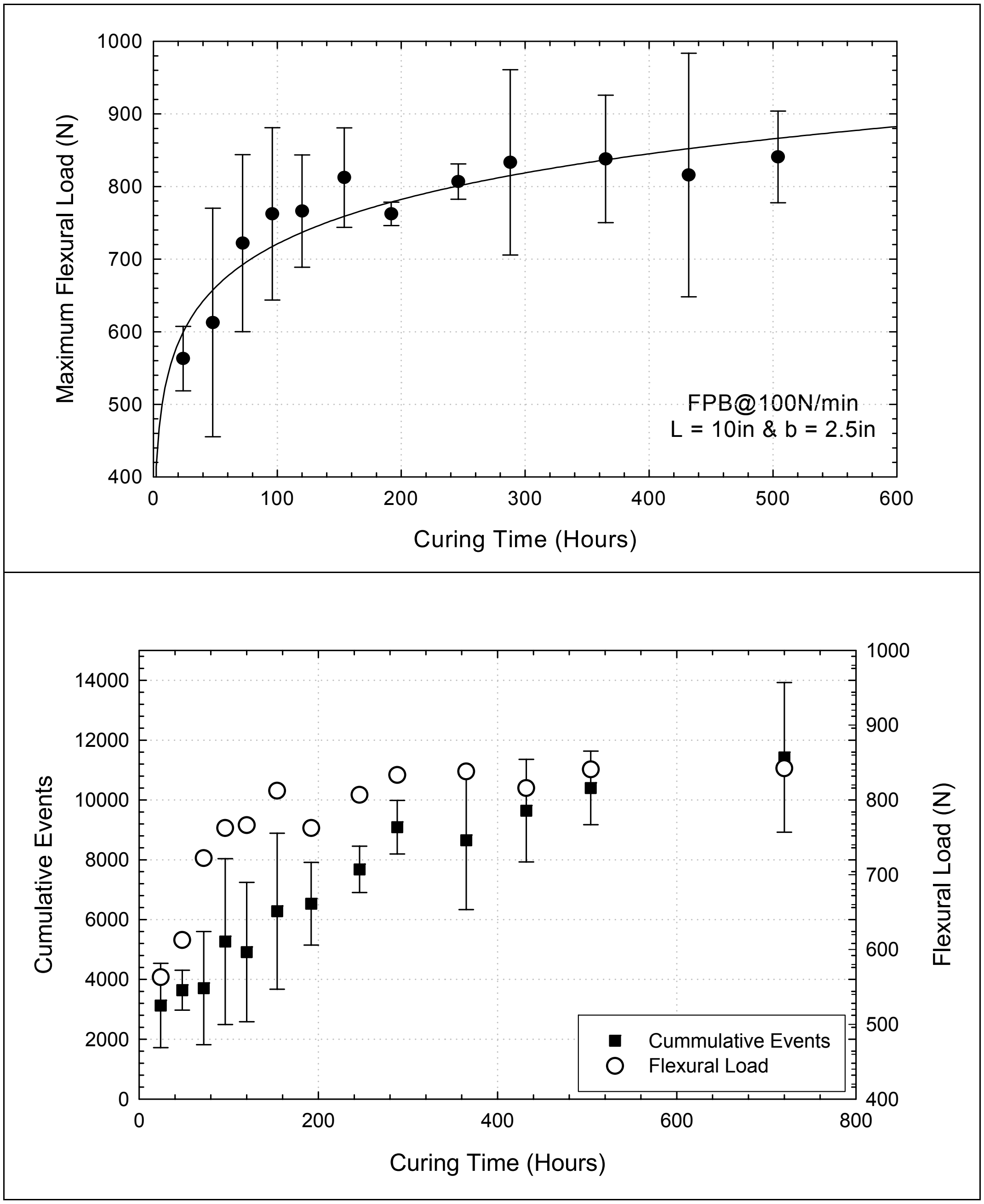

Figure 7: a) Flexural strength as a function of curing time (CT), and b) cumulative AE evens and strength as a function of CT, error bars refer to the standard deviation

With the analysis of AE events, amplitude, energy level and position, damage were classified in various constituents of the sandwich composite, such as core and facesheets as shown in Table 3. Amplitude and energy levels were found to be independent of the loading type for the sandwich composite used. To confirm AE damage classification results, various preliminary tests were terminated at certain AE amplitude and energy levels. Specimens were carefully removed, dissected and analyzed microscopically to confirm AE sequence of failure given in Table 3. This classification qualitatively matched well with the damage sequence reported in the literature [26, 39-41]. Care must be exercised in interpreting AE parameters and graphical presentations as AE figures represent dynamic, time marching data that is updated continuously throughout the duration of the test.

Fig. 9 shows a typical load-deflection curve to three different cutting time, as increases the curing time the failure mode tends to sudden and brittle. Fig. 10 shows irreversible evolution of AE activity from low (core damage and inherent specimen defects accommodation) to high AE activity corresponding to fiber rupture leading to catastrophic failure.

Table 3: AE sequence of failure and corresponding amplitude and energy ranges for sandwich composites, under fatigue and static test

Failure Mode	Amplitude (dB)	Energy (Marses)
Core Damage	30-60	0-20
Interface failure and Resing cracking	50-80	0-12000
Resin and fiber rupture	50-90	0-25000

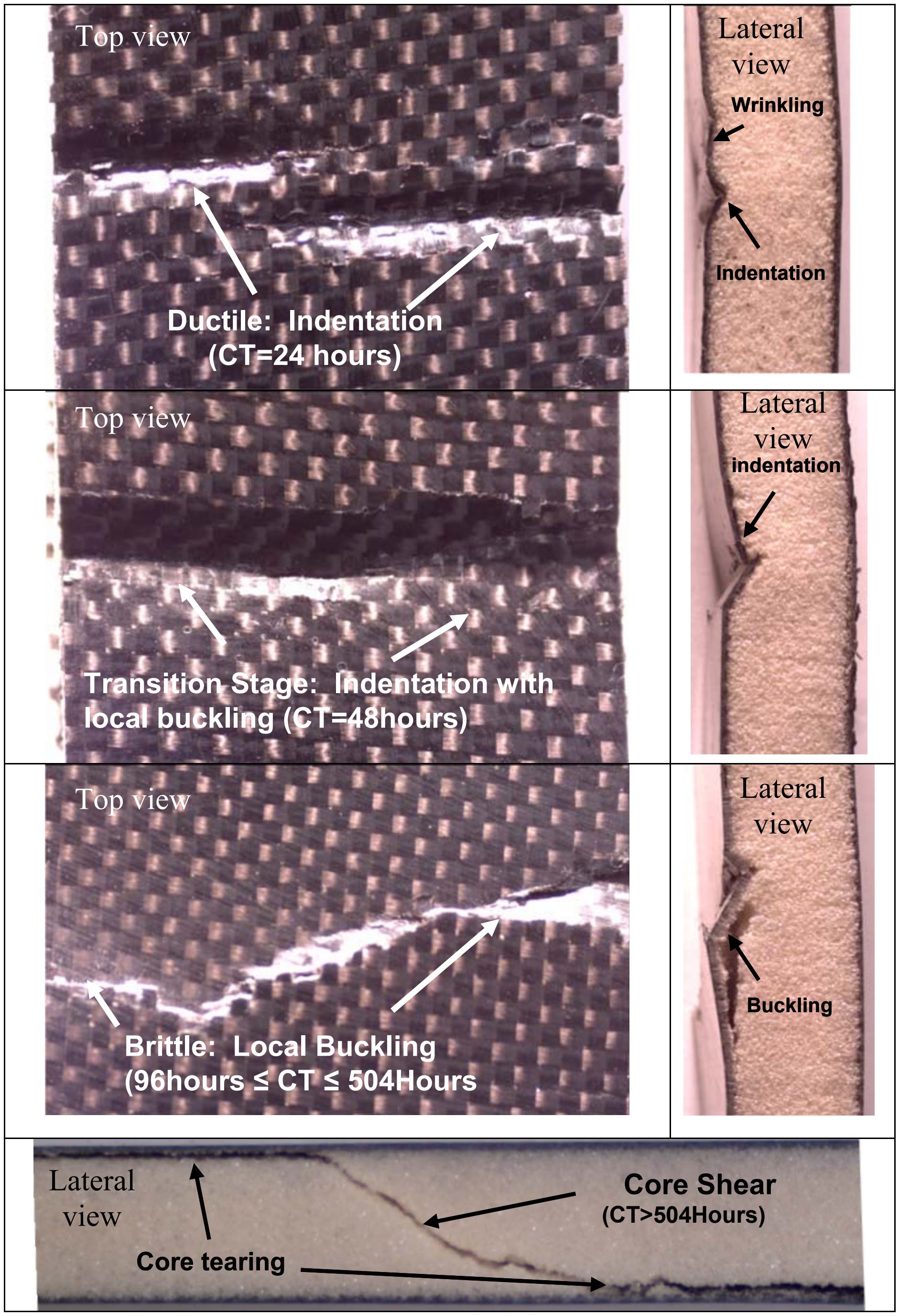

Figure 8: Top and lateral view of ductile to brittle failure mode as a function of CT on sandwich composites

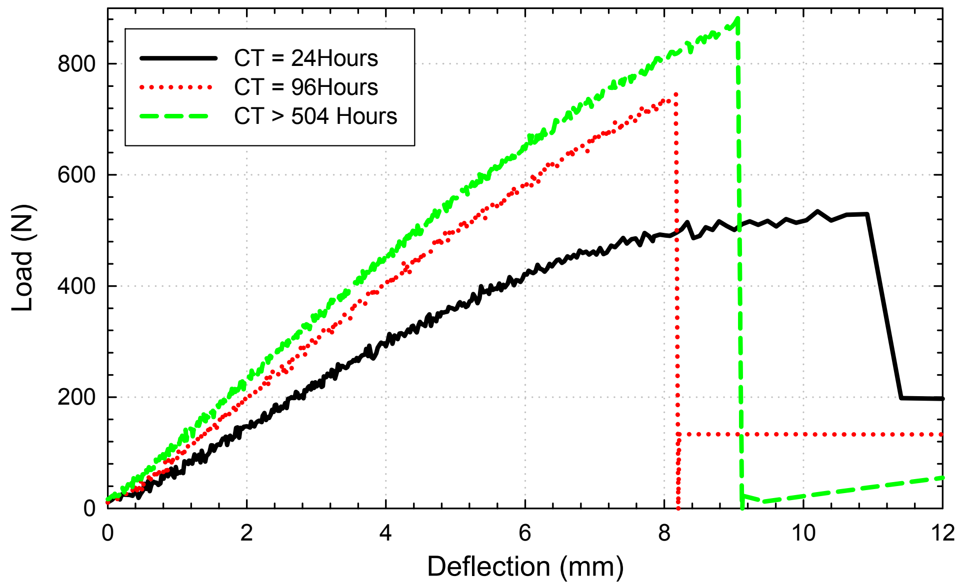

Figure 9: Typical load-deflection curves for sandwich composite for different CT

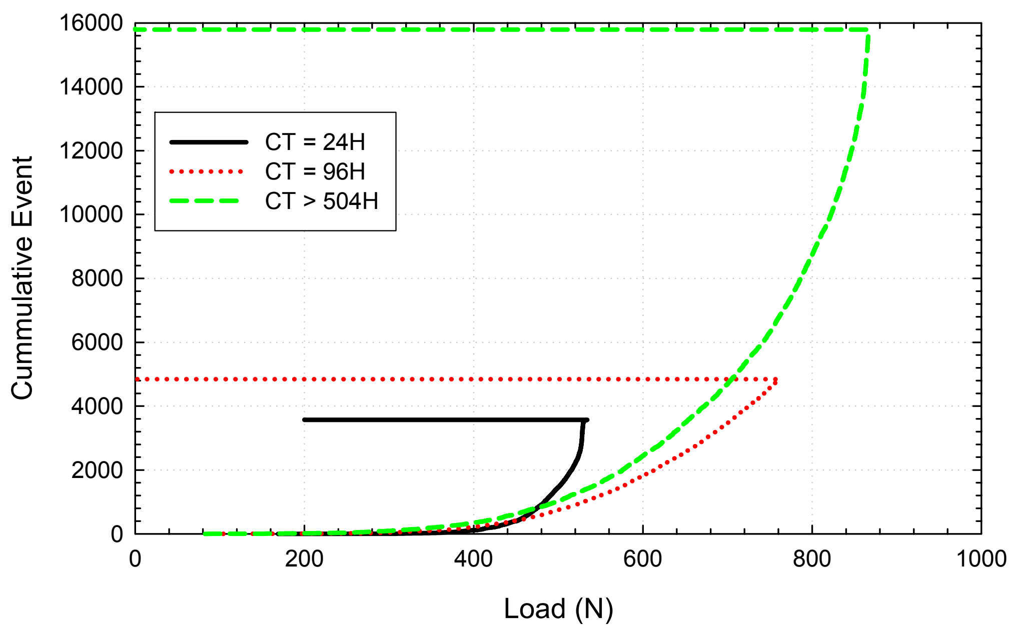

Figure 10: Typical cumulative AE event under static loading for sandwich composite for different CT

4.1.1 Quasi-Static Flexural Characteristics

The loads in the sandwich composites are primarily carried by the high stiffness carbon fiber facesheet whereas an order of magnitude softer core serves to enhance toughness and the bonding agent is responsible for the maintenance of two-phase action of the composite. The mean load-displacement along with standard deviation curve shown in Figure 11 depicts an apparent linear and reversible behavior leading up to the catastrophic failure. However, it must be realized that this load-displacement behavior primarily reflects the load carrying capability of the facesheet. AE analysis provides evidence of core and interfacial failure long before any indication of facesheet cracking (Figure 12), therefore, the curves shown in Figure 11 may not be reversible in reality.

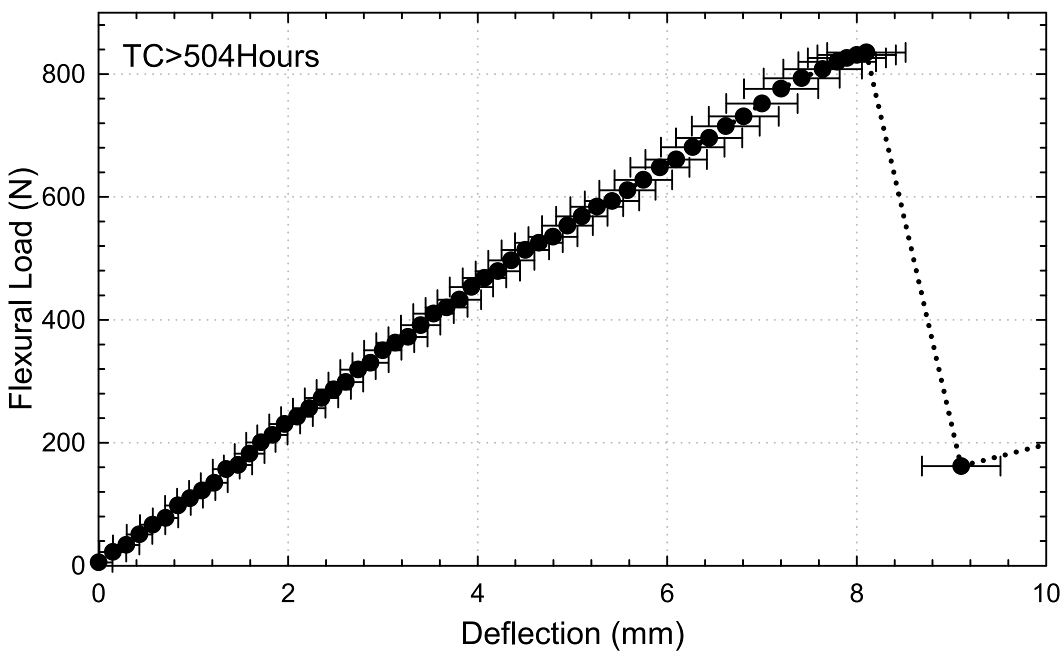

Figure 11: Static flexural behavior of fully cured sandwich composites, error bars refer to the standard deviation

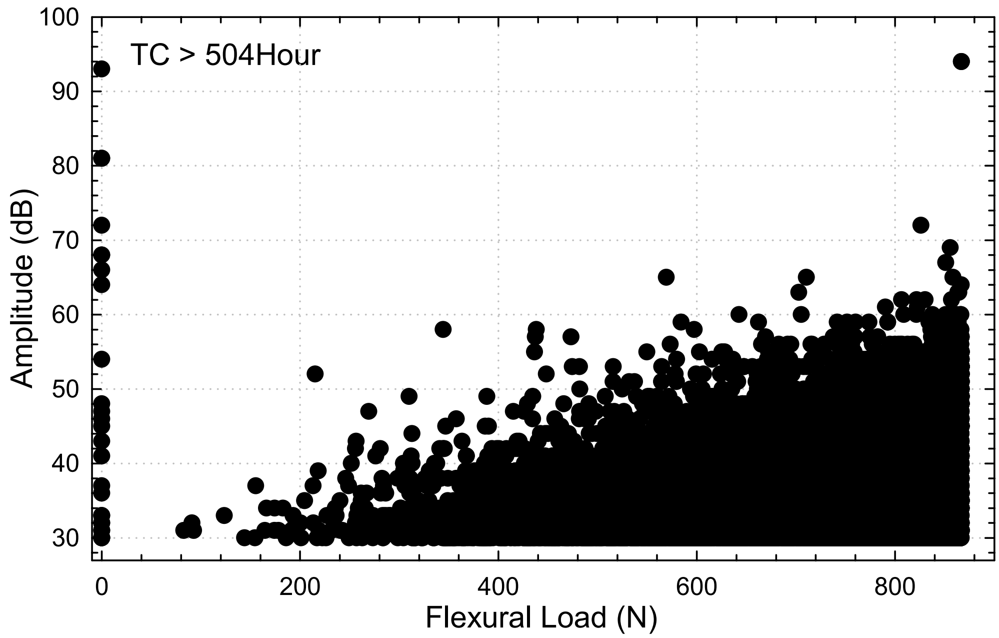

Figure 12: Typical AE activity under flexural loading of fully cured sandwich composite beam.

The initial portion of the load-displacement curve up to the yield point of the weakest constituent of the sandwich composite (i.e., the core) yielded very quite AE region for all specimens tested, perhaps associated with the incubation period. Thereafter, data suggested a sequential progression of AE activity as the test proceeded. Figure 12 (amplitude vs. load) shows typical AE activity as it relates to amplitude of occurrence with the corresponding classification of failure.

According to AE results (such as Figure 12) core failure invariably initiated near the interface with the facesheet at the lowest energy level and dominated the earlier part of testing by gradually propagating along the interface (core tearing) and through the thickness direction (core shear). Post-failure analysis of various specimen types indicated that the resin cracking was not wide spread, as most of the core-facesheet separation was caused by a planar core tearing (in the plane of specimen surface) near the facesheet as show in Fig. 13.

Substantial weakening of the foam core and the interface led to the onset of facesheet rupture and catastrophic failure. However facesheet activity was largely absent prior to catastrophic failure. Somewhat similar results have been reported in the literature [47].

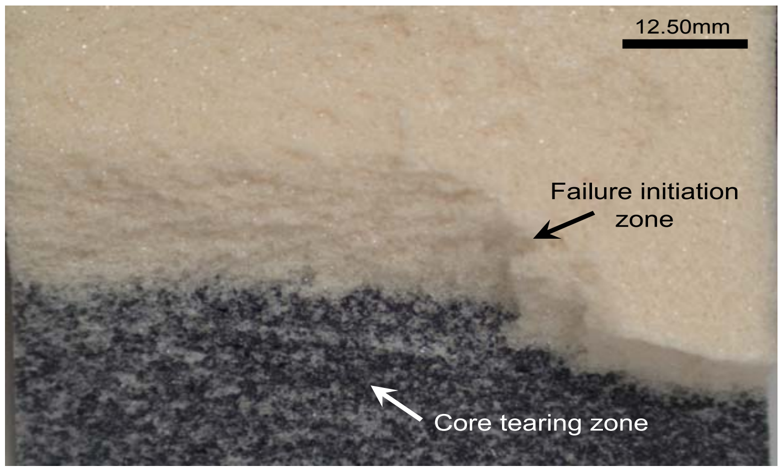

Figure 13: Failure surface under static flexure test shows core tearing, shear, and failure nucleation zone

The level of AE amplitude and energy were found to be independent of the specimen geometry or loading type for the sandwich composite used. AE figures represent dynamic, transient data that is updated continuously throughout the duration of the test. Data shown in Figure 12 (amplitude vs load) provides an overall AE statistics during the indicated load value; using the value obtained in Table 3 the core damage activity occurred 97% of the time whereas fiber breakage consumed only 3% of the typical static testing time.

4.2 Fatigue Characteristics

A spike in the AE activity was observed in the initial period of testing perhaps corresponding to specimen accommodation and release of residual stresses, etc. that subsided within a few thousand cycles of testing as detailed in Fig.14. However, this initial AE activity did not correspond to any discernable cracking in the sandwich composites. The failure was observed to be primarily of core shear that caused the delamination between the facesheets and the core that led to catastrophic failure due to facesheet rupture (Fig. 15). A large part of fatigue life damage was consumed by the core failure activity whereas catastrophic failure was sudden and abrupt. Failure process was not visible through any optical means and the only damage information that was obtained came from the in-situ or post failure AE and microscopic analysis. Somewhat similar failure sequence has been reported in the literature [26-28, 40, 45]. For flexural fatigue tests on sandwich composites, however, unlike the reported results significant fiber rupture never took place until catastrophic failure in the current study. Test results indicated the formation of a single crack front that suffered periodic growth and frequent intermittent dormant intervals as evidenced by AE analysis. Figure 15 shows a typical failed specimen.

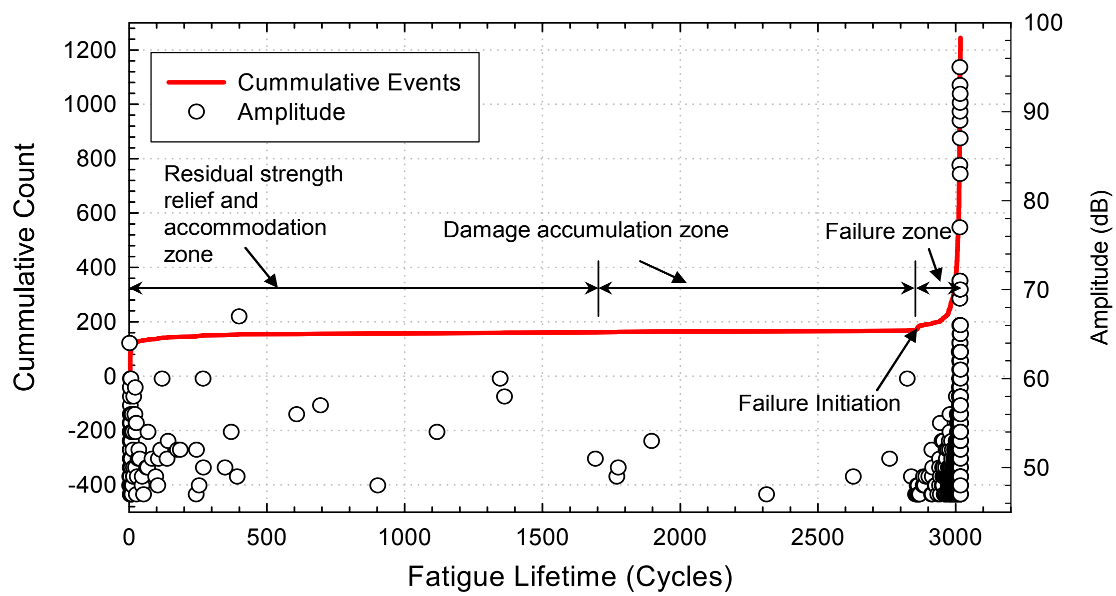

Figure 14: AE activity during the fatigue lifetime ($P_{max} = 0.9P_{ult}$)

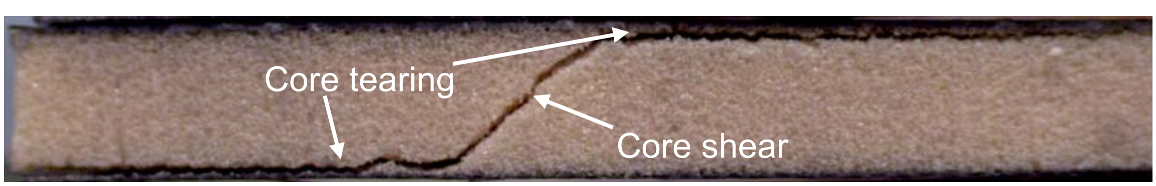

Figure 15: Core shear failure under fatigue experiment along the sandwich composites thickness

Increasing stress level corresponded to increased deflection as indicated by the maximum deflection vs normalized fatigue lifetime curve shown in Figure 16. The normalization was performed with respect to the fatigue lifetime of each maximum load applied. S-N curve shown in Figure 17a, b indicates a decrease in lifetime as a function of increasing stress level. In the current study, no significant failure activity occurred in any constituent of the sandwich composite at stress levels below 60% which also coincided with the 500,000 cycle threshold. The literature does not list a clear endurance limit for sandwich composite, however, flexural fatigue life has been reported as low as 60% of the ultimate static load [27]. The high endurance limit, though based on somewhat lower cutoff, may be attributed to superior bonding of the facesheets to the core that made it difficult to initiate the crack in the core or at the interface. Furthermore, multiple crack initiation sites during the initial stage of testing may have dissipated energy, thus effectively reducing stress intensity required for a single crack to form and propagate.

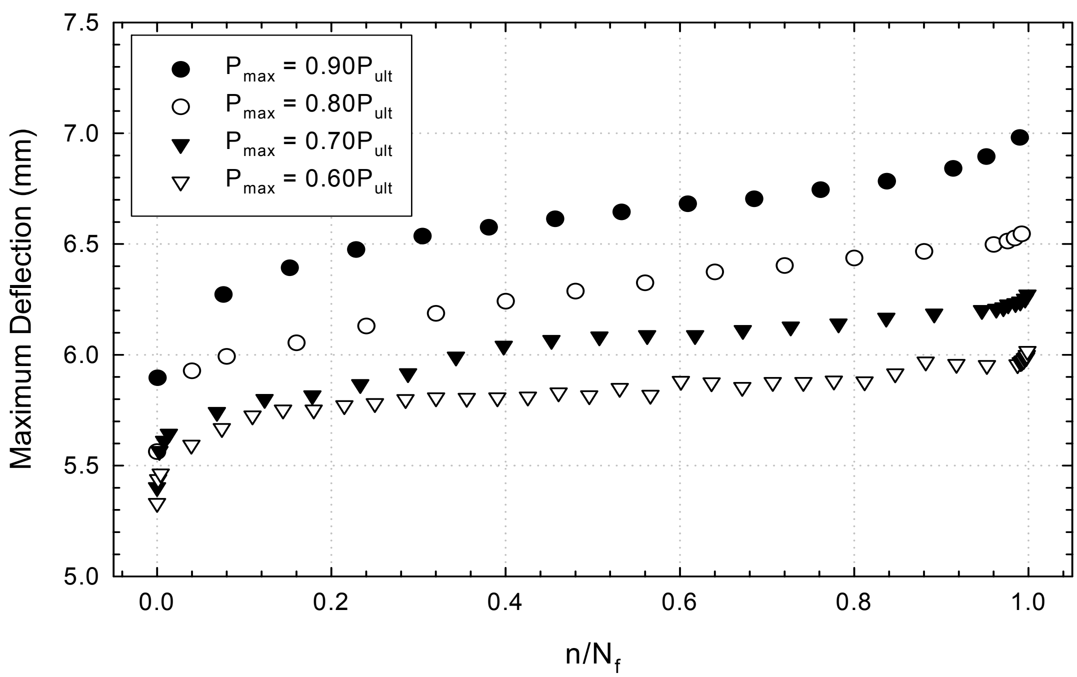

Figure 16: Maximum deflection measured along the normalized fatigue lifetime

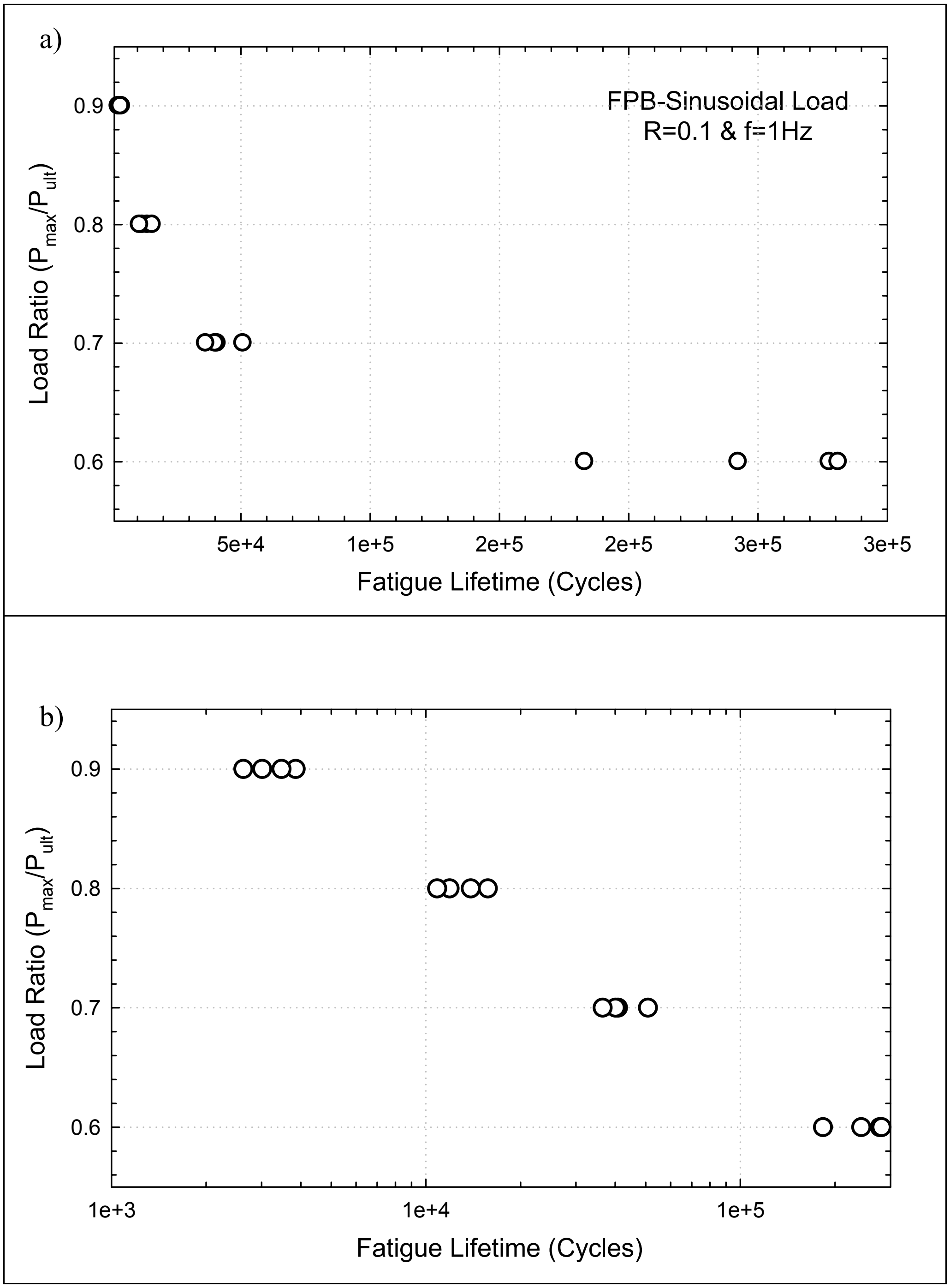

Figure 17: S-N curve of foam core sandwich composites a) arithmetic scale, and b) semi-logarithmic scale

Increasing stress level also lead to increased AE activity. However, almost independent of the stress levels, AE analysis consistently indicated a predominant single major crack front initiating in the core and shearing through the core shear while localized within a 10mm radial zone near the point of application of the load. In some cases, AE pointed to multiple crack initiation fronts in the interface however, only one major crack formed and propagated through the core. The dominant crack was also found to tear the core along the interface before propagating through the core.

Catastrophic failure was preceded by almost sudden and significant fiber rupture that lead to severe facesheet stiffness reduction. This stage was arrived at after substantial weakening of the multi-phase action that exists among various constituents of the sandwich composite, mainly as a result of damage to the core and the interface. Lifetime results obtained in the current study qualitatively compared well with the reported sandwich composite fatigue characteristics, however, adequate quantitative differences were observed as expected, as the different material systems and loading parameters were used in the current study [26-28, 45].

5 SINGLE AND REPEATED SLAMMING OF HONEYCOMB CORE SANDWICH COMPOSITE PANELS ON WATER [52]

This chapter presents the results of the polyester foam filled honeycomb core sandwich composite, detailed in Table 1a.

5.1 Results and Discussion

5.1.1 Single Slam

In single slam tests, a substantial reduction in post slamming flexural strength was observed; however, the reduction in strength did not follow a clear pattern as a function of slamming energy. The results of non-slammed and the three zones of the single slam specimens compared in Figures 18 and 19 clearly indicate that the maximum loss of strength to occur in zone 3 (near the chine). According to the test results, catastrophic/apparent failure was observed between 892N-m and 1020N-m of slamming energy. Post slamming flexural tests reveal that significant damage took place even at a very low slamming energy level that left no visible/apparent damage to the sandwich composite specimen. Some scatter in the observed data was mainly attributed to inherent and fabrication flaws.

The strain results showed a swift rise followed by a gradual decay at each strain gauge location, except where catastrophic failure occurred, as shown for typical cases illustrated in Figures 20a, b (refer to Figure 5 for strain gauge numbering). Figure 21 shows a comparison of typical strains obtained as a function of slamming energy; higher slamming energies appear to boost the strain magnitudes slightly, whereas for each specimen the highest strain magnitudes were found along the free edges. Figure 21 also illustrates decreasing strains along the slam direction, therefore, indicating maximum strains to occur in zone 1 of the specimen that incidentally also coincides with the location of peak pressures, as seen in Figure 22, however, contrary to intuitive expectation, where least loss of strength is observed (Figure 19). It is worth noting that the peak pressure and strain times do not coincide perhaps as it takes time to overcome inertia of the material, which is consistent with the reported results [8, 9]. The strain results are quite useful and relevant; however, caution must be exercised in their analysis as the measurements depend quite deceptively on the relative location of strain gauges with respect to the damage site.

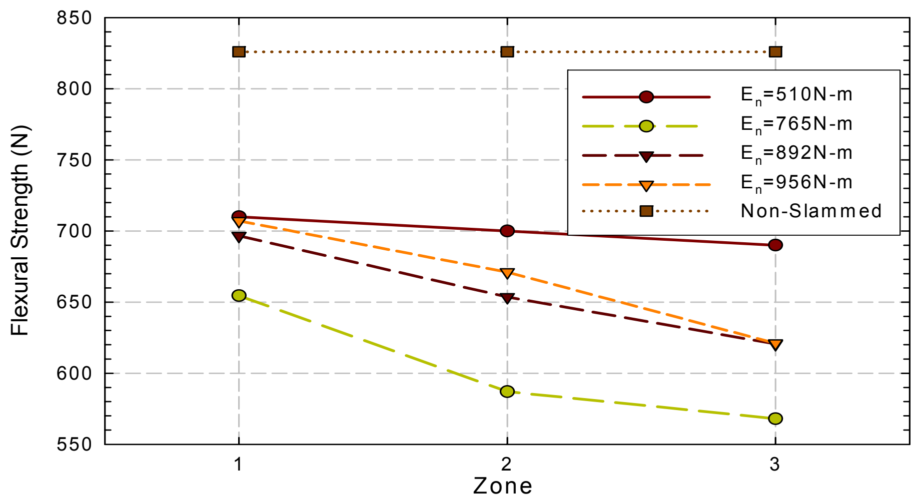

Figure 18: Remaining flexural strength of non-slammed and slammed specimens as a function of pressure zones

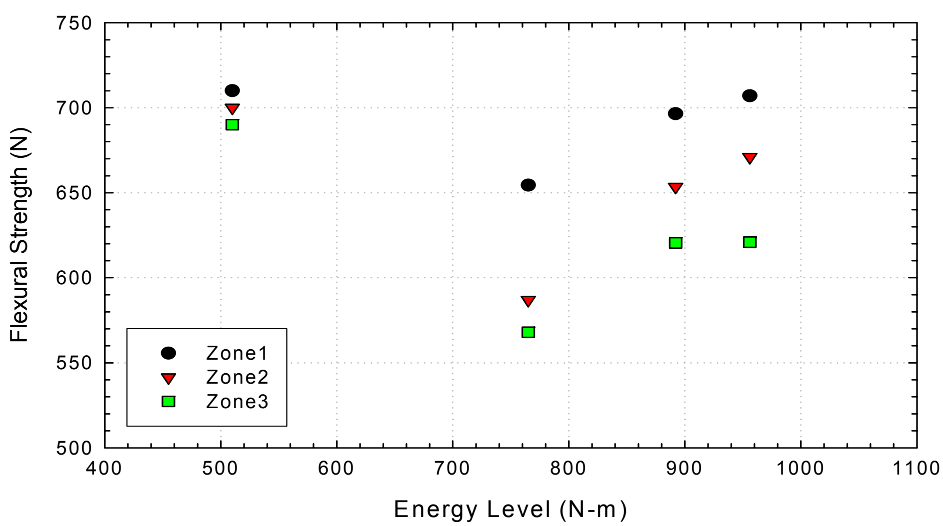

Figure 19: Remaining strength of slammed specimens as a function of slamming energy

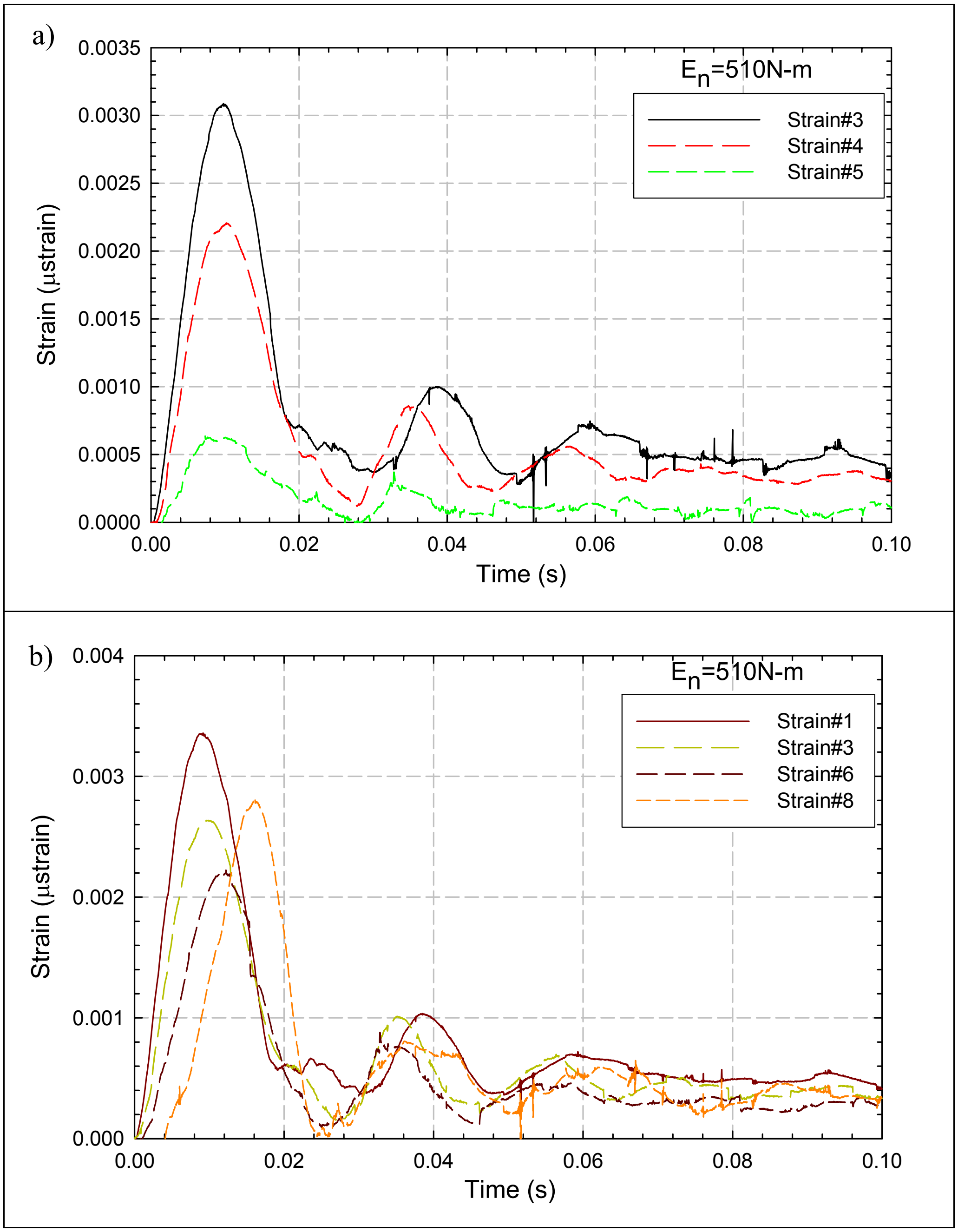

Figure 20: Typical strain results obtained from single slam, a) span direction, and b) slam direction

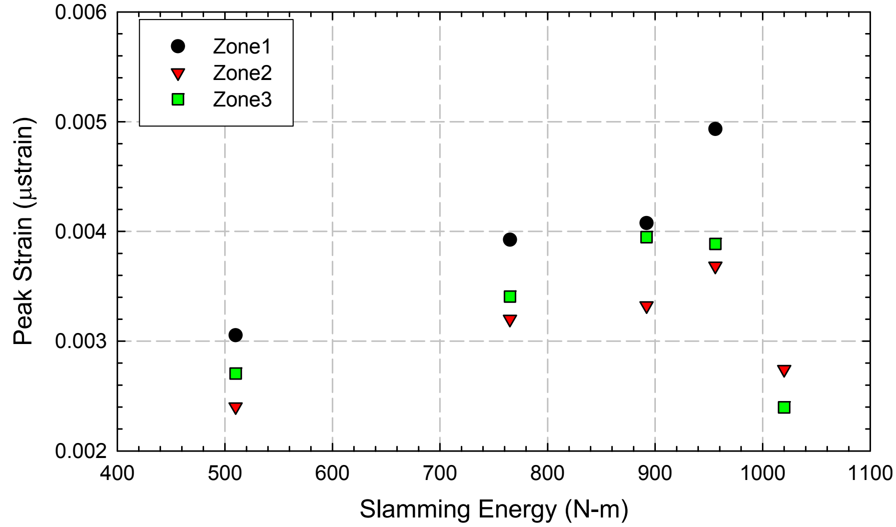

Figure 21: Average peak strains along the slam direction as a function of slamming energy

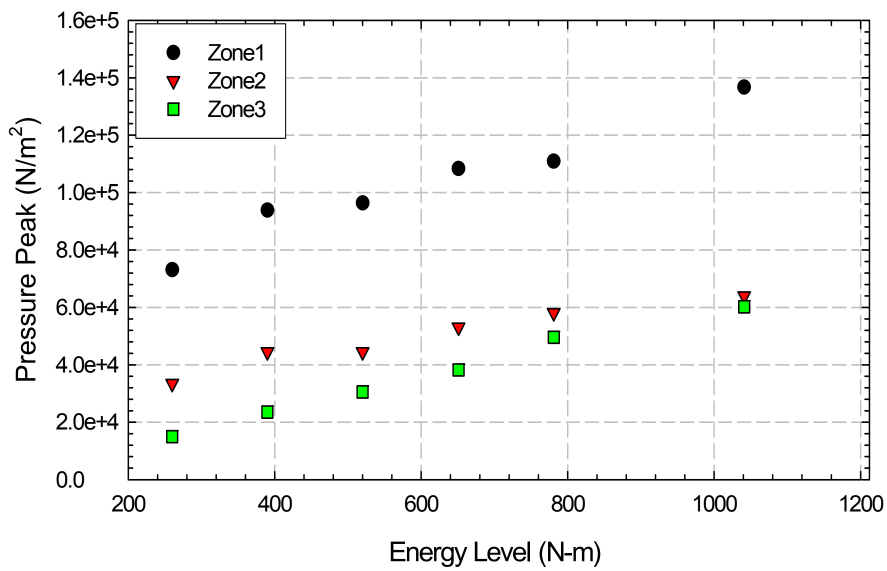

Figure 22: Average peak pressures along the slam direction as a function of slamming energy

It is interesting to note that the highest strain and pressure readings were obtained in zone 1 (near the keel) of the specimen while the maximum loss in strength due to slamming consistently occurred in zone 3 (near the chine), Figures 19, 21, and 22. The current results agree with the literature on the peak pressure and strains occurring near the keel under free drop conditions [10, 11, 15]. It is, however, difficult to reconcile with the idea that location of peak pressure and strain do not coincide with the location of maximum damage under free drop conditions. Under constant velocity experiments [4, 14], it is easier to reason why chine could possibly suffer greater damage by for example, noticing that if pressure is integrated over the whole panel including the pressure peak at the chine, greater overall pressure at the chine as compared to the keel is obtained. However, under free drop, the pressure at the chine is dramatically lower than at the keel (Figure 22), therefore, the same idea if followed, would still result in overall greater pressure at the keel.

Since the velocity of slamming pulse propagation is substantially higher than the velocity of crack propagation, when a compression pulse is incident on a free boundary it gives rise to a reflected tension pulse. Therefore, it can be argued that as soon as the keel impacts the water, a wave is generated that travels in various directions including towards the free edge of the chine, where it is immediately reflected as a tensile wave. So that immediately after reflection, the tensile stress (or momentum) gains twice the magnitude it had at the head of oncoming pulse. The reflected part of the pulse travels back to the source and is reflected back again towards the chine. The interface of such reflected pulses may give rise to very complicated stress distributions and superposition of several reflected pulses may produce stresses which are sufficiently large to cause increased damage near the chine. The complicated physical mechanisms are not yet completely understood. Particular difficulties are experienced in delineating slamming impulse, energy absorption and wave propagation and reflection which are responsible for such a behavior. However, it should be noted that the ship design is based primarily on peak pressure measurements that may be obtained near the keel or the chine depending on the deadrise angle (and constancy of velocity) with the presumption that the critical damage must coincide with the same location as evidenced by several theoretical and experimental [5, 7, 9, 11, 20, 24, 48].

Detecting damage during the actual slamming event is a very difficult task. In the current effort, acoustic emission sensors were used in post slamming flexural tests in order to ascertain damage sustained during slamming. Under flexural testing, AE results clearly indicated a reduced time to failure in slammed specimens as compared to the non-slammed specimens, as illustrated in Figure 23. It is curious to notice that even though the overall amplitude and energy levels remained the same for failure in each constituent of the material (as AE signatures are a function of material properties), the overall number of acoustic events reduced measurably from an average of 2300 events for non-slammed specimens to about 1100 events in the slammed specimens (Figure 24) - zone 3 showing a measurably lower activity and time to failure as compared to zone 1 (Figures 23 and 24) – thus corroborating the remaining strength results shown in Figure 19. AE analysis also aided in quantifying cumulative damage as exemplified in Figures 25. Damage causes a quantitative reduction in AE activity and the same damage event can't repeatedly emit an acoustic signal (Kaiser's effect), therefore, by analyzing cumulative AE activity during the post slamming flexural tests, the accumulated damage during the slamming event can be deduced, as seen in Figures 25. By taking the difference in cumulative AE activity curves, a quantitative measure of damage under slamming can be established. Furthermore for polyester foam filled honeycomb core sandwich composite, the facesheet failure, core shear, core crushing, interface failure and indentation, etc. all correspond to a discernable AE amplitude and energy level; e.g. facesheet failure occurred over 60dB amplitude while core failure occurred within a range of 35-45dB. AE, therefore, offers a reliable post slamming quantitative tool to ascertain the otherwise obscure slamming induced accumulated damage in the material. Similar to the difficulties observed in Figures 19 and 21, the AE results, however, did not offer a clear trend in the AE activity as a function of slamming energy, perhaps due to the inherent flaws and scatter that is generally observed in the material [2, 5, 9].

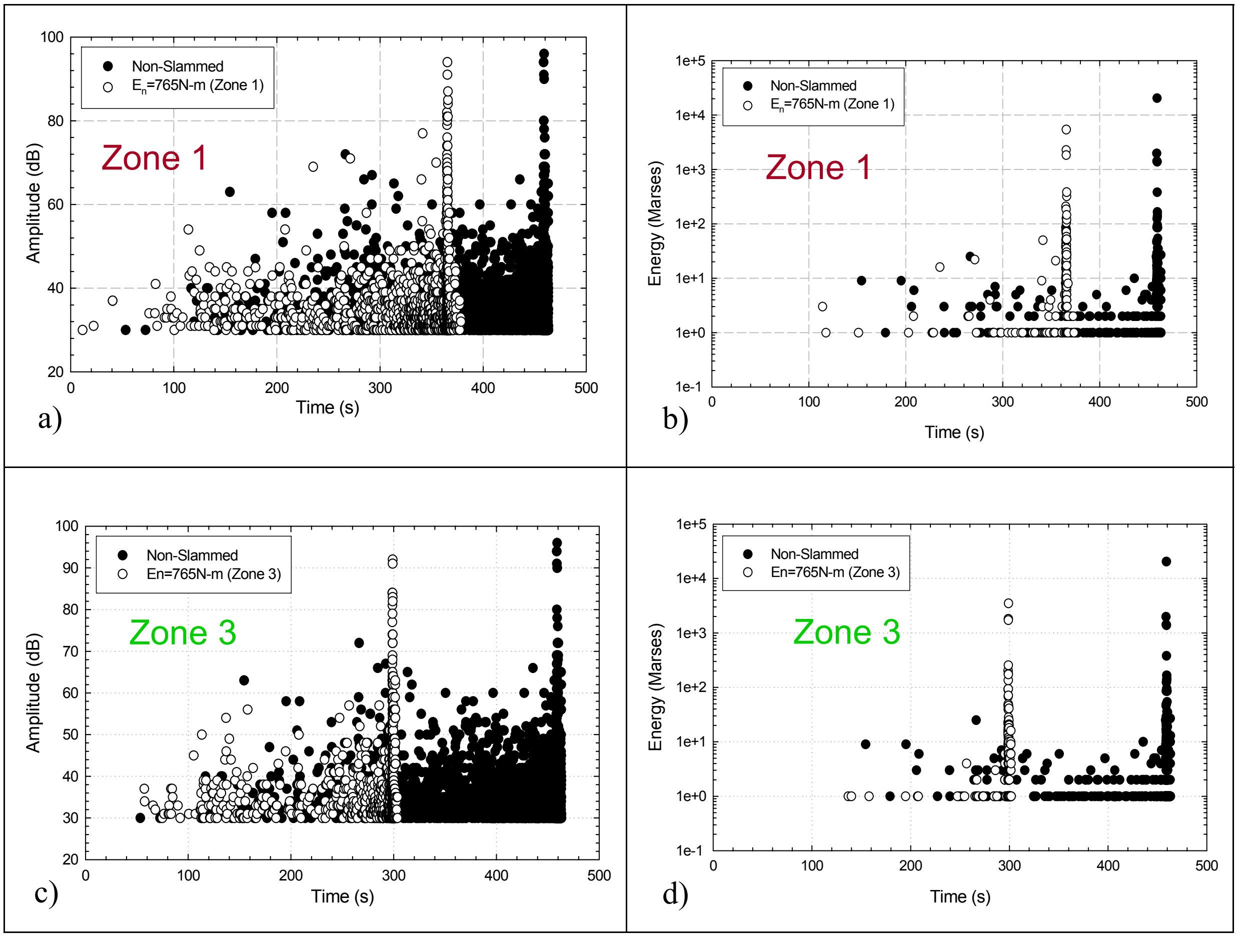

Figure 23: Typical AE amplitude and energy results of non-slammed and slammed specimens during the static testing, a) and b) high pressure zone, c) and d) low pressure zone

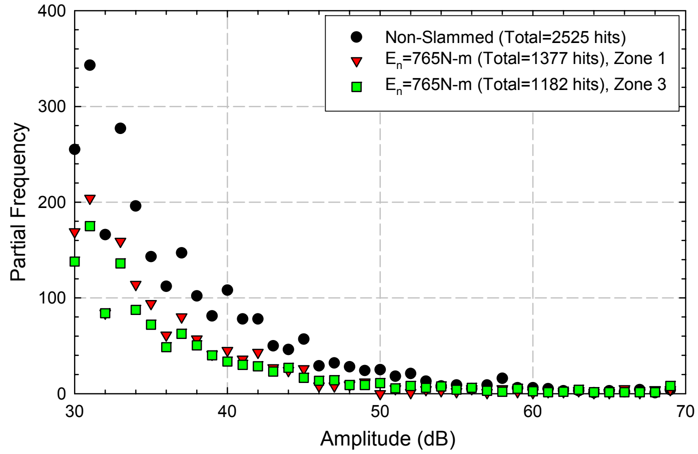

Figure 24: Comparison of recurrence of AE event as a function of amplitude of non-slammed and slammed specimens

a)

b)

c)

d)

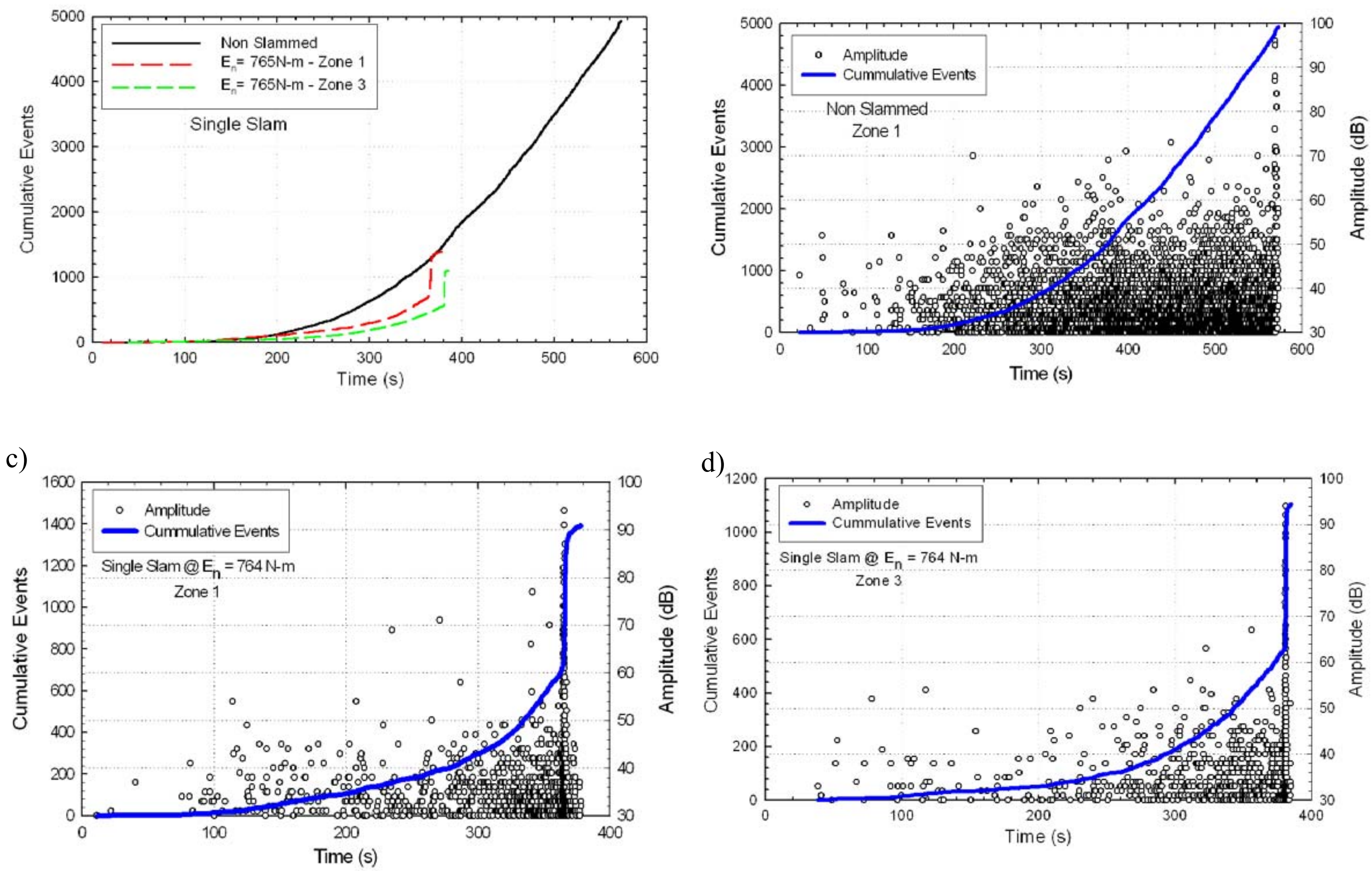

Figure 25: Cumulative and amplitude distribution of AE event observed for a typical specimen of non-slammed and slammed specimens, a) Cumulative events, b), c), and d) Cumulative event and amplitude correspond to each event

Based on strain data during slamming, visual inspection and post slamming microscopic analysis and flexural tests monitored by AE, face yielding was observed to be the predominant mode of failure of the facesheets, whereas local crushing of the foam filled honeycomb core as opposed to global shear failure was identified as the primary mode of failure. Figure 26 shows a typical micrograph of a specimen with no apparent damage during slamming, cut into three zones and tested under flexure. The dominant crack followed a curved path matching in three zones during post slamming flexure, as seen in Figure 26. Whereas, another specimen tested shows three distinct crack (paths) indicating no crack formation under slamming, as seen in Figure 27.

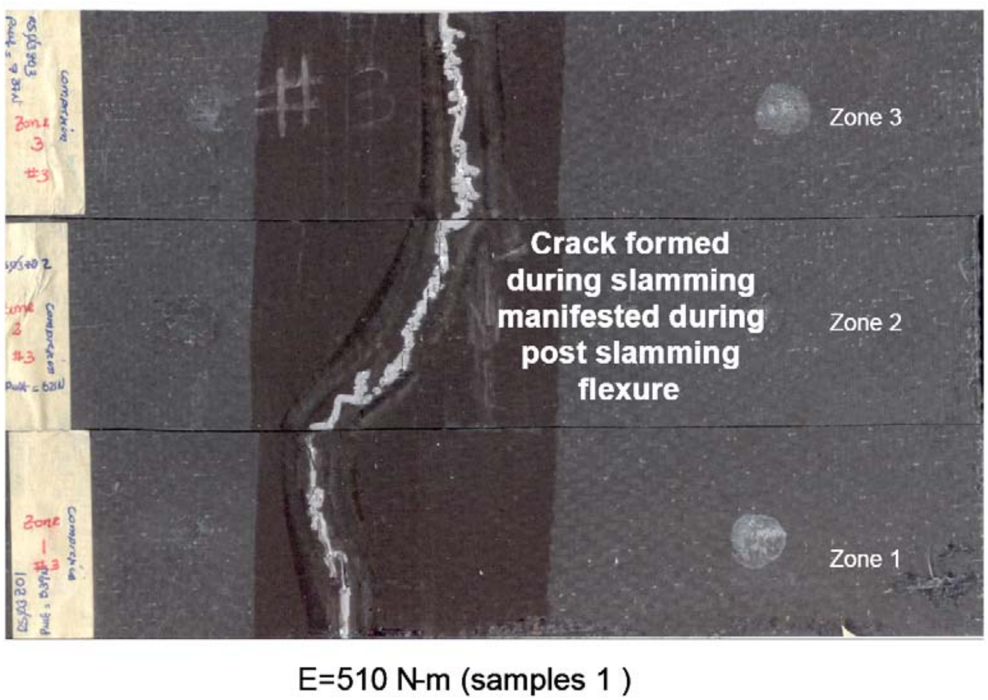

Figure 26: Dominant crack induced during slamming and revealed during post slamming flexural.

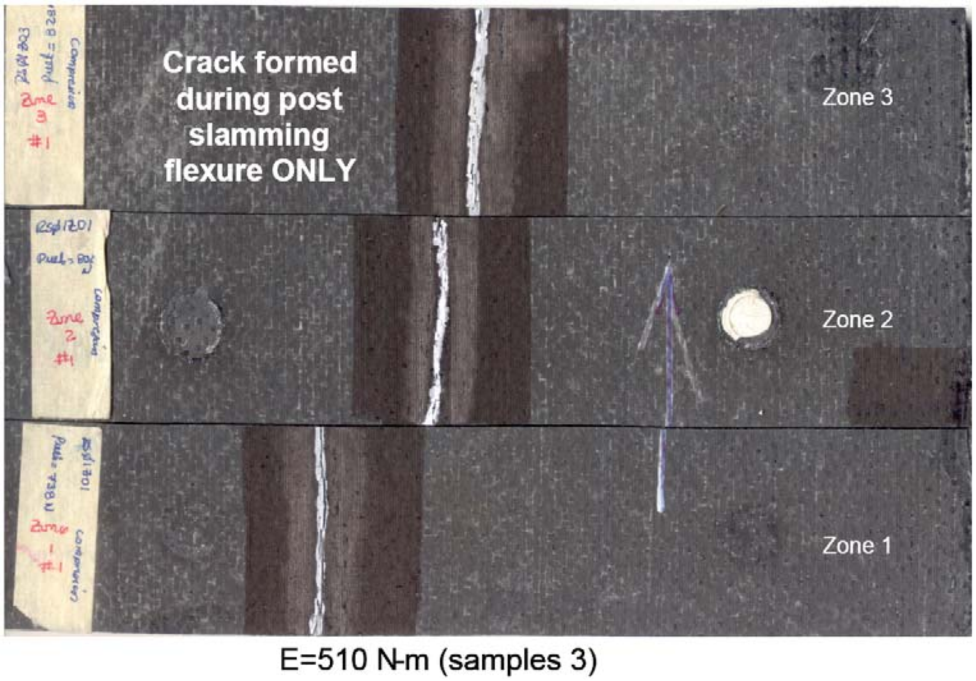

Figure 27: Crack formed and propagated during post slamming flexural test.

5.1.2 Repeated Slamming

The main objective here was not necessarily to induce catastrophic failure (or to obtain number of cycles to failure), but rather to understand damage progression, accumulation and modes of failure. Therefore the repeated slamming was performed for an arbitrarily selected 50 cycles. The testing was performed at various slamming energy levels ranging from 50% to 75% of ultimate slamming energy to failure (E_{ult}) obtained under single slam scenarios. At 75% and beyond, all specimens failed catastrophically within less than 5 cycles. Increasing lifetime was obtained with decreasing slamming energy below 75% of E_{ult}. At 50% E_{ult}, none of the specimens failed within 50 cycles, however, post slamming flexural tests indicated widespread damage that resulted into a significant reduction in lifetime and major crack formation with the hallmarks of slamming induced crack, similar to Figure 26. The results of repeated slamming along with the corresponding post slamming strengths are tabulated in Table 4.

Under repeated slamming, pressure did not appear to change cyclically as it is a function of slamming energy only. The strain on the other hand did exhibit irregular/inconsistent changes but there was no clear trend that could point to crack formation or growth as a function of number of cycles or slamming energy.

Table 4: Repeated Slamming Results

Energy Impact [N-m]	Type of Experiments		Slamming Fatigue Life [cycles]			
			Sample 1	Sample 2	Sample 3	
510	Slamming Lifetime		**>50**	**>50**	**>50**	Average
	Remaining Strength [N]	Zone 1	738	748	593	**693**
		Zone 2	802	732	621	**718**
		Zone 3	828	713	737	**759**
637	Slamming Lifetime		**41**	**>50**	**>50**	Average
	Remaining Strength [N]	Zone 1	-	757	724	**741**
		Zone 2	-	758	572	**665**
		Zone 3	-	751	626	**689**
701	Slamming Lifetime		**24**	**12**	**38**	
>750	**Failed within 5 cycles**					
			Non-Slammed Average [N]			**826**

Similar to single slam tests results, peak pressure and strain were obtained near the keel, however, unlike single slam, maximum damage was not always found near the chine. Under repeated slamming, the widespread cyclic damage accumulation perhaps obscures the maximum damage sites (in various zones) that were observed under single slam scenario. It is nevertheless interesting to notice again that the location of peak pressure did not necessarily coincide with the location of maximum damage. The results of damage in various zones can be seen in Table 4.

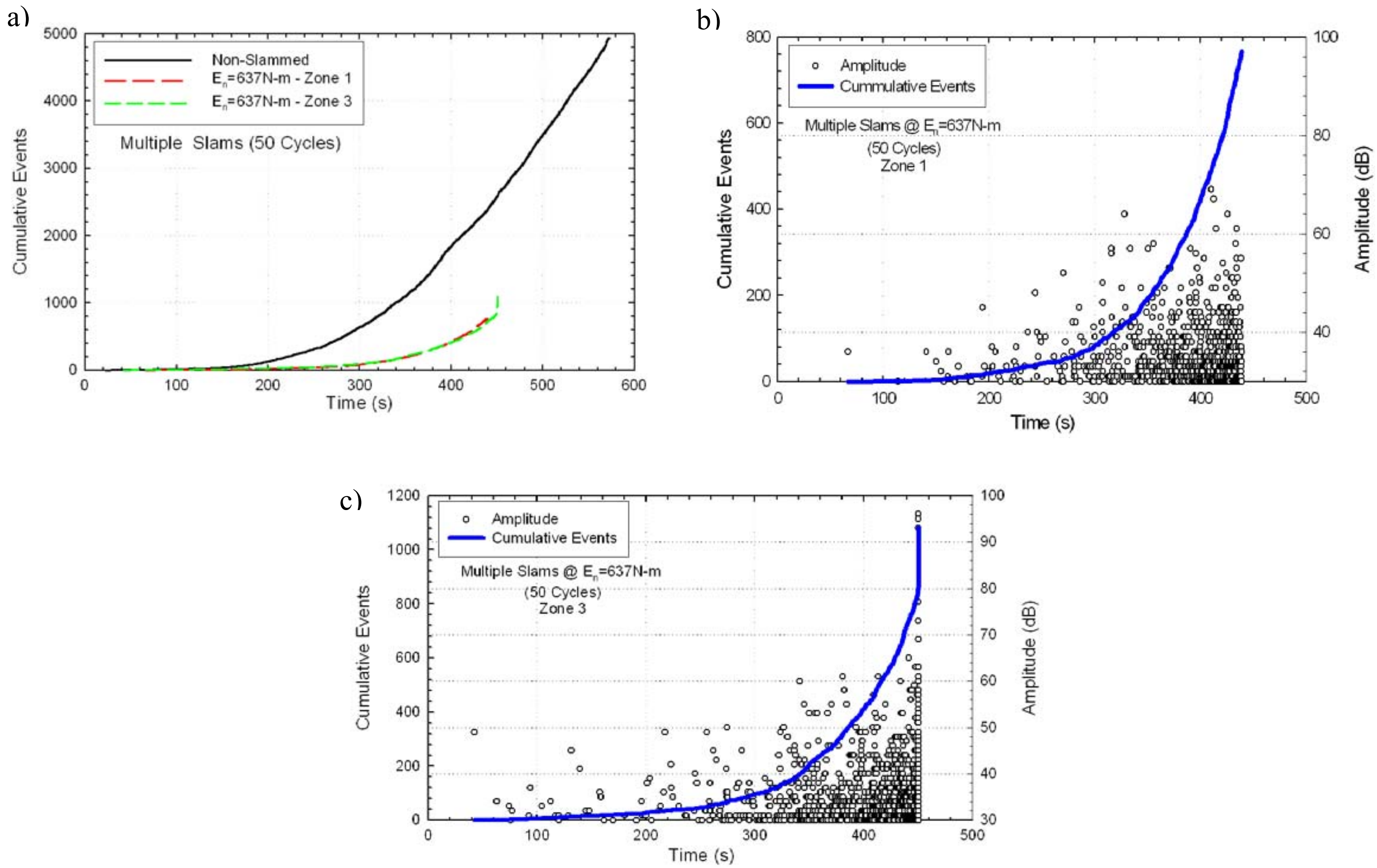

Figure 28: Cumulative AE activity results from static flexural test of a typical non-slammed and multiple slammed specimens, a) Cumulative events, b) and c) Cumulative events and amplitude of each event.

AE technique was once again employed to assess the damage accumulation and discern modes of failure under repeated slamming. Changes in AE activity at various amplitude regimes provided a quantitative measure of the state of damage in the material. The cumulative AE activity shown in Figure 28 clearly indicates a significant reduction in AE activity for a typical specimen slammed for 50 cycles. Figure 29 shows a comparison of cumulative AE activity of typical non-slammed, single slam and multiple slam specimens. Clearly, repeatedly slammed specimens exhibit the greatest damage as compared to non-slammed and single slam specimens.

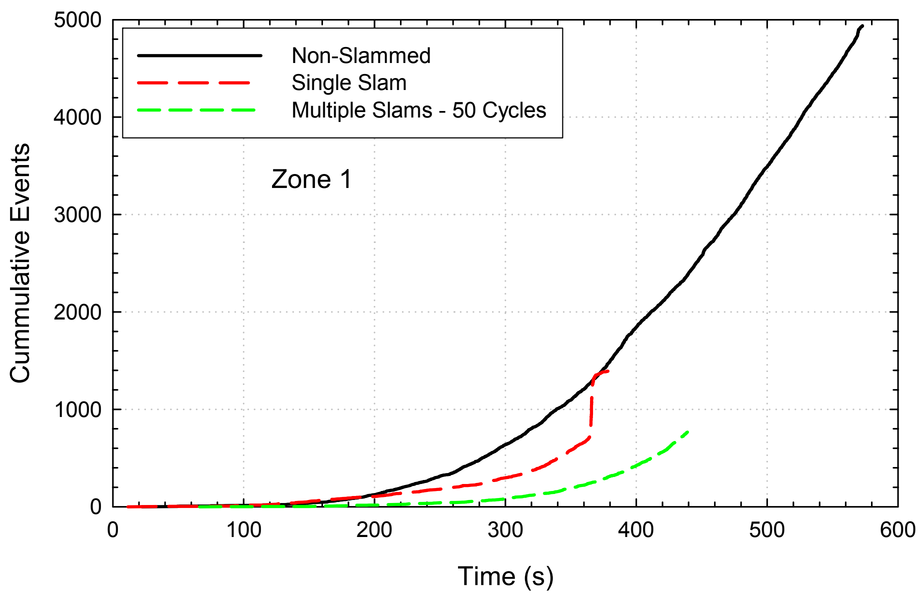

Figure 29: Comparison of cumulative AE activity under static test of a typical non-slammed, single slammed and multiple slammed specimens at 637N-m of slamming energy.

6 SINGLE SLAMMING OF FOAM CORE SANDWICH COMPOSITES [58]

This chapter presents the results of single slam of polyurethane foam core sandwich composites considering the effect of: deadrise angle (β) and slamming energy E_n.

6.1 Results and Discussion

Table 5 summarizes the test results as a function of deadrise angle β and slamming energy E_n. As anticipated, a decrease in β and an increase in E_n increases the probability of failure, that is in accord with the principle of conservation of momentum and trends reported in the literature [11, 15]. Pressures measured at various β 's and E_n's as shown in Figure 30 compared favorably with the standard Wagner/Von Karman type theoretical solution; note that Eqs. 1 and 2 yield infinite pressure at $\beta = 0^o$ while a finite pressure is obtained experimentally. Literature is heavily focused on slamming pressure measurements, being the principle design parameter [9, 12, 49, 50], however, it offers very little in terms of understanding damage mechanisms or associated failures. Strains on the other hand, though providing discrete information, currently appear to be the best choice for in-situ damage assessment [6, 11]. The critical information corresponds to the peak strain magnitude and the strain rate in the initial transient stage; while the subsequent strain readings correspond mainly to the deformation recovery and damping phase, as seen for typical cases presented in Figures 31a,b. The peak strain and strain rate results are also consistent with the data shown in Table 5 that exhibits an increasing trend towards failure as a function of decreasing β or increasing E_n (Figures 30).

The maximum strains obtained along the centerline of the span in the impact direction are compared for various β 's in Figures 32(a-d). These plots show slightly higher strains closer to the keel as compared to strains at other locations on the panel, however, there is no clear trend. On the other hand, plots summarizing peak strains for specific sensors along the impact direction (sensors 1,3,6,8, refer to Figure 5) clearly indicate a decreasing trend as a function of increasing β, as seen in Figures 33(a-d). It should be noted that the sandwich panels consistently failed at a strain beyond ~0.0035mm/mm. It is expected that the threshold strain will depend strongly on the material system used and the boundary conditions.

Table 5: Percentage of specimens failed catastrophically as a function of slamming energy (En) and deadrise angle (β)

	Deadrise Angle (β)			
Slamming Energy, E_n (J)	**0°**	**15°**	**30°**	**45°**
161	20%	0%	0%	0%
269	100%	0%	0%	0%
386	100%	0%	0%	0%
511	100%	67%	0%	0%
642	100%	100%	0%	0%
779	100%	100%	33%	0%

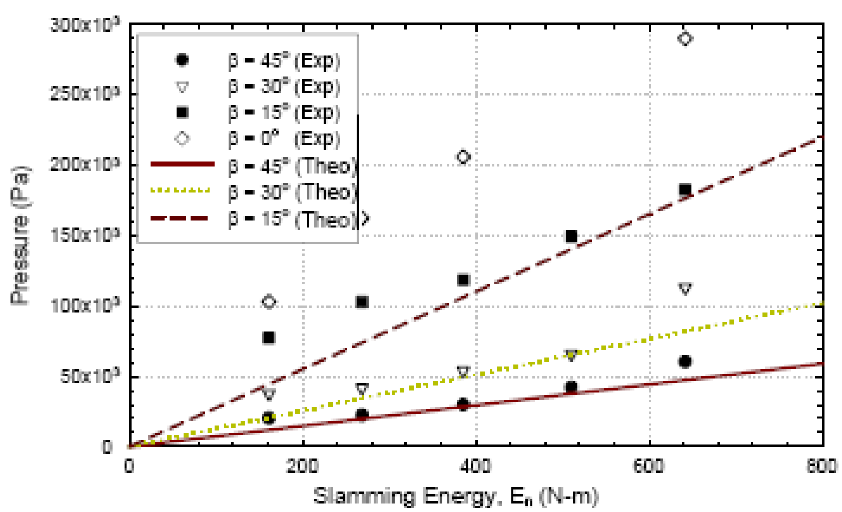

Figure 30: Experimental pressure distribution profile compared with the analytical pressure distribution.

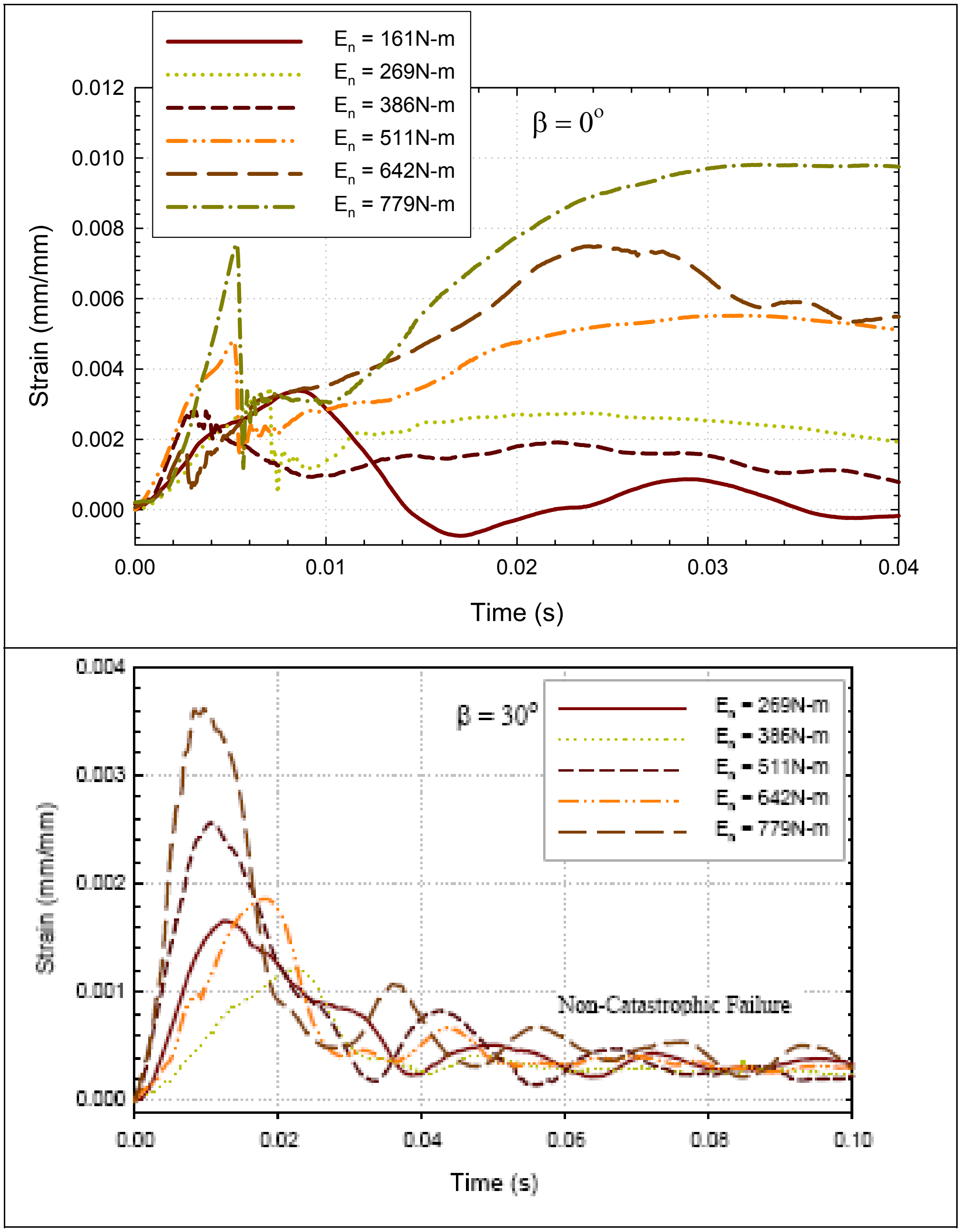

Figure 31: Transient strain profiles obtained during slamming (strain sensor 1 located at 13mm from keel along the middle of span) of typical specimen, a) β = 0°, b) β = 30°

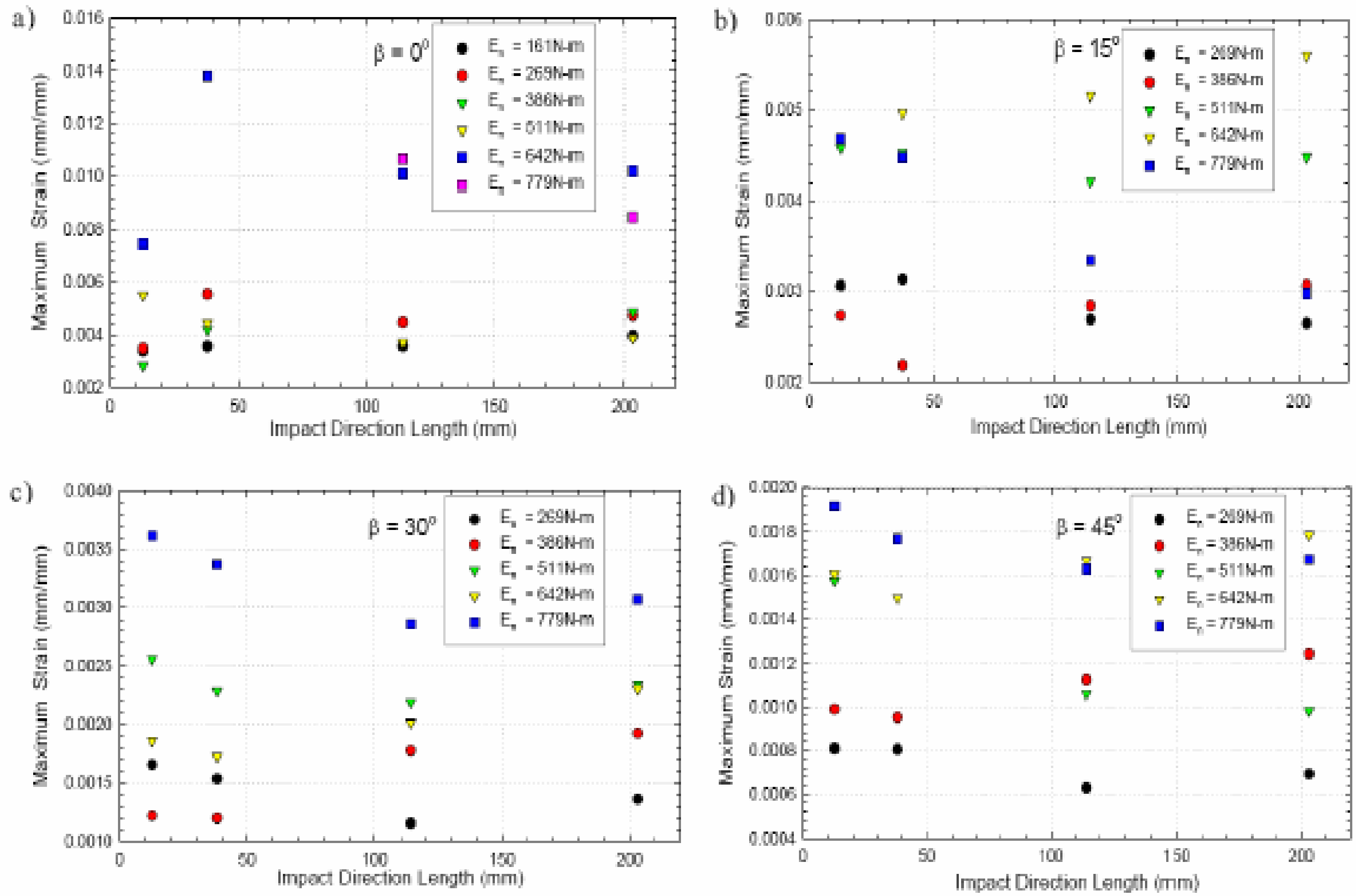

Figure 32: Peak strains obtained along the impact direction (Strain gauges 1, 3, 6, 8), a) $\beta = 0^o$, b) $\beta = 15^o$, c) $\beta = 30^o$, and d) $\beta = 45^o$

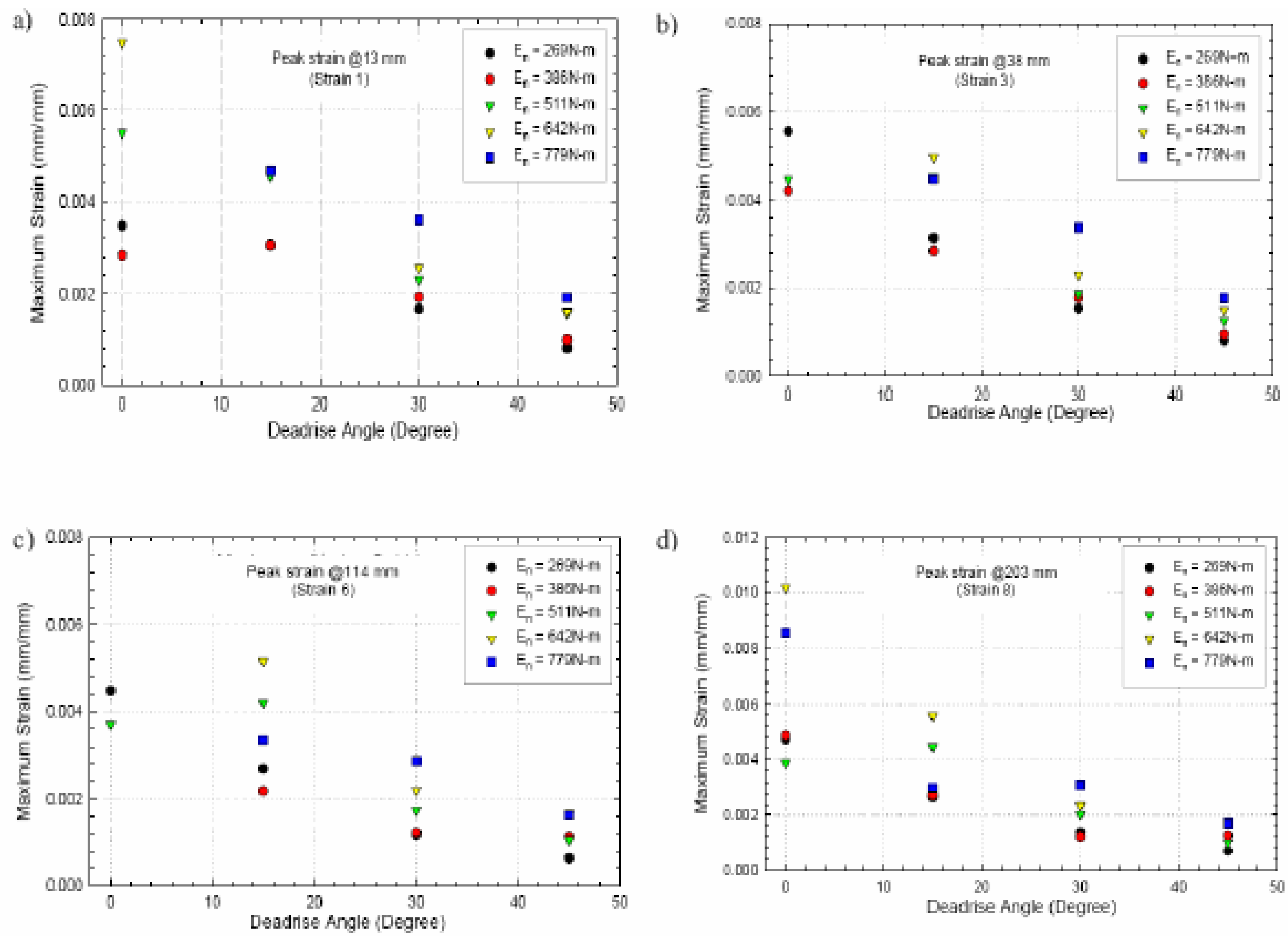

Figure 33: Peak strains as a function of dead rise angle obtained at specific location, a) strain 1, b) strain 3, c) strain 6, and d) Strain 8

It is evident from Figures 30-33 that the increment in β reduces the panel deformation under the same slamming energy; similarly an increase in E_n increases the strain for a constant β. These results are qualitatively in accord with the analytical and experimental observations reported in the literature [4, 6, 9, 11, 20, 51]. In order to make a quantitative assessment, peak experimental strains were compared with theoretical strains derived by making quasi-static assumption and applied to simply supported panel with average distributed pressure taken from Wagner's theory (Eq. 1 [9, 15]). The theoretical strain ε can then be written as

$$\varepsilon = \mu_H \frac{\rho_w b y \pi^2 L^2 E_n}{16MD\tan(\beta)} \tag{4}$$

where the hydroelasticity function is

$$\mu_H = \frac{\varepsilon_{\exp}}{\varepsilon_{r/q-s}} = 1 - \eta\left[\left(\frac{2E_n}{M}\right)^{1/2}\frac{1}{V_s}\right] \tag{5}$$

and the stiffness of the sandwich composite [46] is,

$$D = E_f\frac{bt_f^3}{6} + E_f\frac{bt_f d^2}{2} + E_c\frac{bt_c^3}{12} \tag{6}$$

Here t_f and t_c correspond to the thickness of the facesheet and the core, respectively, b is the width of the specimen, L is the span length and y is the distance from the neutral axis. ρ_w represents the density of the water; M is the inertia (mass) of the slamming (assembly), whereas E_f and E_c correspond to the modulus of elasticity of the facesheet and foam core. $\varepsilon_{exp}/\varepsilon_{r/q-s}$ refers to the ratio of the experimental strain to the strain obtained using rigid quasi-static assumption. Without including the effect of hydroelasticity (μ_H), the strains were grossly overestimated especially at higher slamming energies, however, the comparison between experimental and theoretical strains improved dramatically when the hydroelasticity function μ_H (Eq. 5) was introduced in Eq. 4, as seen in Figure 34. μ_H which is a function of experimentally adjusted parameter "η ", slamming energy 'E_n' and surface wave propagation velocity 'V_s' of the sandwich composite panel, was developed based on the numerical comparisons of the effects of hydroelasticity provided in the literature [15]. The use of Eq. 4, when applicable, is convenient as it bypasses the complexities involved in the setup and solution of coupled non-linear differential equations.

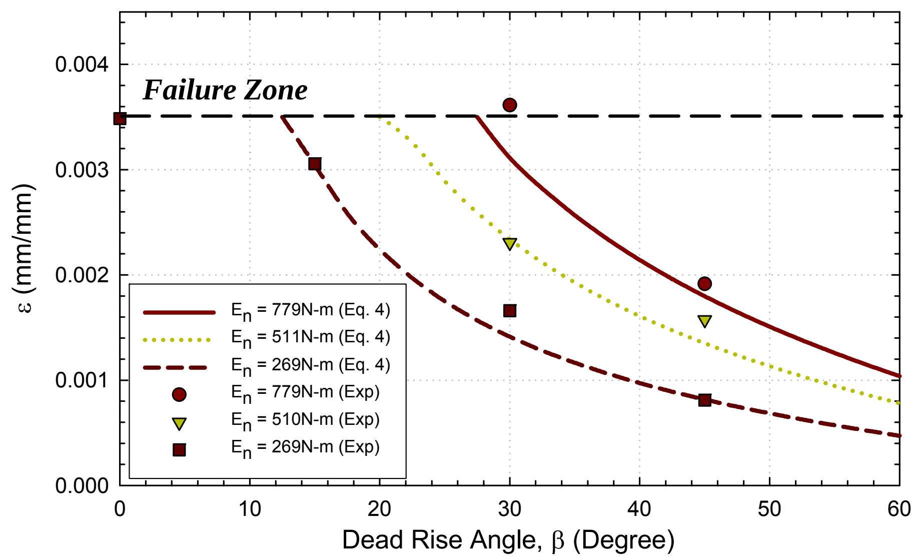

Figure 34: Experimental peak strains compared with theoretical values obtained from Eq. 4.

Transient strain measurements offer valuable damage information; however, in order to ascertain accumulated damage during the slamming process, the non-catastrophically damaged slammed specimens were subjected to quasi-static flexural load. Based on the flexural test results and for the material system used, it appears that under single slamming anything short of catastrophic failure did not induce significant damage to the specimen. The maximum reduction in strength was observed to be about 8% with substantial scatter in the data such that the flexural capacity of the non-slammed specimens fell within the range of the standard deviation. The literature is quite scarce on the failure assessment of partially damaged specimens under slamming. However, contrary to recently reported results on foam filled honeycomb sandwich panels subject to similar slamming conditions, there was not any appreciable strength reduction in the current testing [52].

This apparent lack of damage response in the non-catastrophically failed specimens appears to be related to the properties of material system used, as the modes of failure strongly depend on the relative properties (ductility/brittleness) of various constituents of the sandwich composites and their interaction with each other. It appears that the facesheets of the sandwich composites used behaved in a significantly brittle manner while being rigidly attached to the core with brittle epoxy, as evidenced by the micrographs shown in Figures 35. It is well known that brittle materials manage to retain their mechanical properties until (near) the catastrophic failure [32, 53]. To further support the observations, the sandwich composites fabricated with the exact same specification except for different curing times were tested under flexure. Figure 9 shows a clear shift in the stiffness resulting from significantly ductile to brittle transition of the sandwich composite as a function of curing time. As the slamming tests were performed after complete curing of 504 hours, the insignificant reduction in the flexural capacity is, therefore, principally attributed to the substantially brittle facesheets and rigid nature of the sandwich composites. A careful comparison of the failure mechanisms under slamming (such as, Figures 35a,b) vividly shows the transition from ductile micro-buckling features to brittle epoxy fragmentation accompanied by fiber pullout/facesheet rupture indicating poor energy transfer to the core before catastrophic failure.

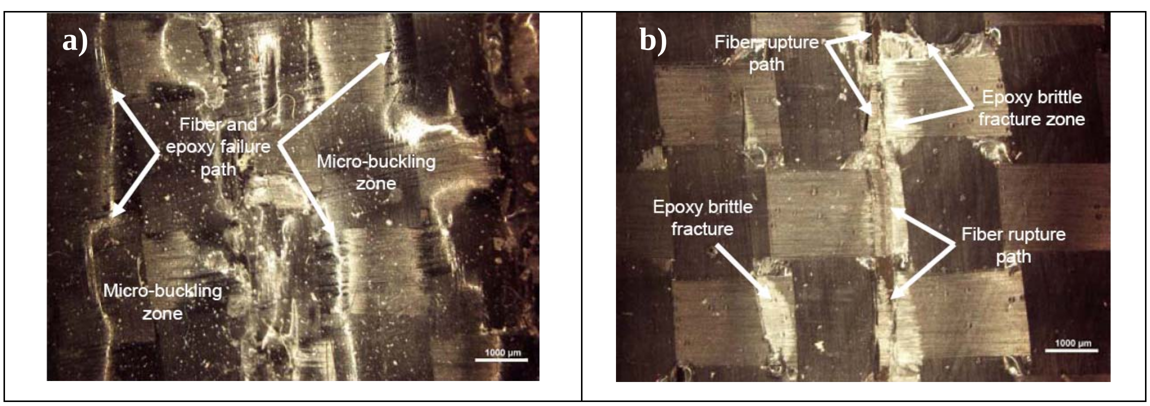

Figure 35: Micrographs showing transition in the failure modes from ductile to brittle as a function of curing time, a) CT = 24 hours indicating ductile failure features, b) CT = 504 hours indicating brittle failure features

A consensus exists in the literature that significant core shear precedes facesheet rupture and catastrophic failure under static or dynamic loading [20, 48, 50]. However, it is difficult to accurately quantify damage in various constituents of the sandwich composite during the slamming process due to the discrete nature of the strain data. The problem is further exacerbated as the slamming process leaves few clues to reconstruct the sequence of failure during a post slamming analysis especially in brittle sandwich composites such as currently used, where damage was largely absent in non-catastrophic cases as indicated by a lack of microscopic evidence of any damage i.e. cell collapse, core shear, resin fragmentation, local buckling, etc. However, the core of specimens with slamming catastrophic failure appear to have suffered substantial shearing along the interface, while there was only sporadic core shear through the thickness as evidenced by Fig. 37a. The facesheets primarily suffered local buckling with some resin fragmentation and final complete failure with fiber pullout. One of the characteristic properties of sandwich composites is their ability to absorb energy; the facesheet functions as the impact controlling parameter while core acts as a cushion that aids in energy absorption. When the panel hits the water, stress waves are generated along the panel, which propagate three dimensionally through the material. The transfer of energy depends significantly on the relative properties and wave attenuation of the facesheet and the core. In the material system currently used, the facesheets appear to be very stiff and bonded to the core with brittle epoxy resulting in a fairly rigid material, therefore, compromising the transfer of energy from the facesheets to the core. As a result, very little damage to the core was observed under single slamming scenario prior to catastrophic failure. On the other hand, under flexure, the failure sequence observed using AE analysis indicated predominantly core shear through the thickness and along the interface with the facesheet proceeded by some resin cracking, causing substantial global weakening and leading to facesheet rupture and catastrophic failure, as seen in Figures 36b.

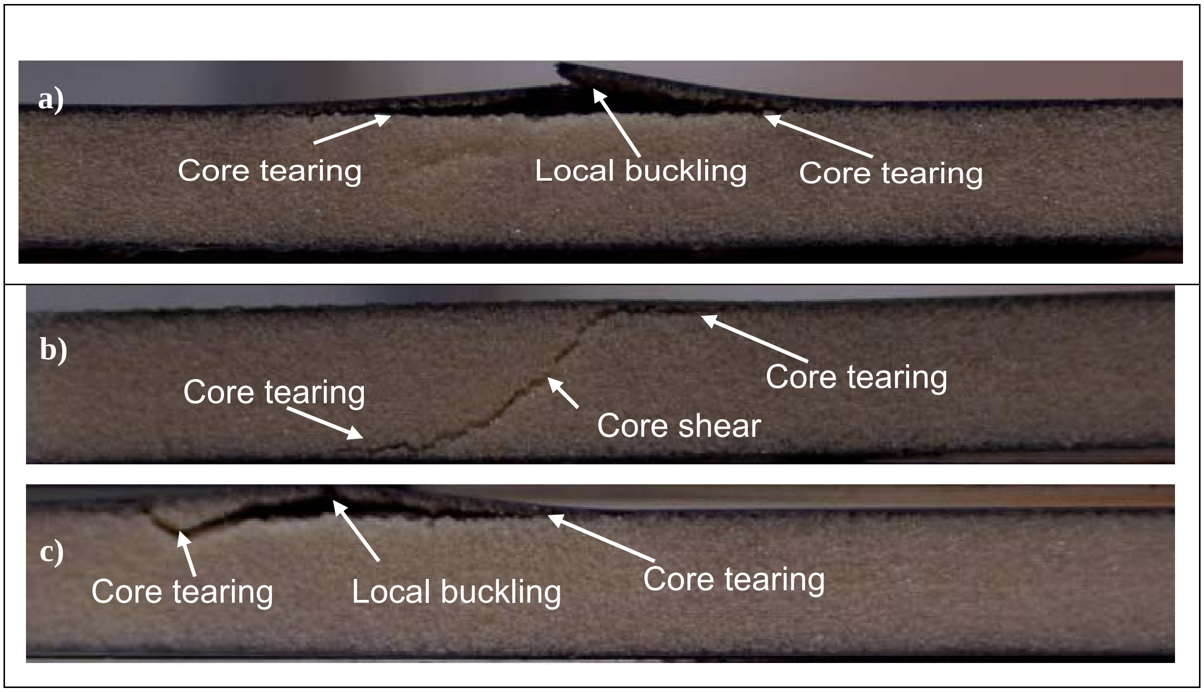

Figure 36: Modes of failure observed, a) local buckling under single slamming, b) core shear under flexure test, and c) local buckling under flexure test

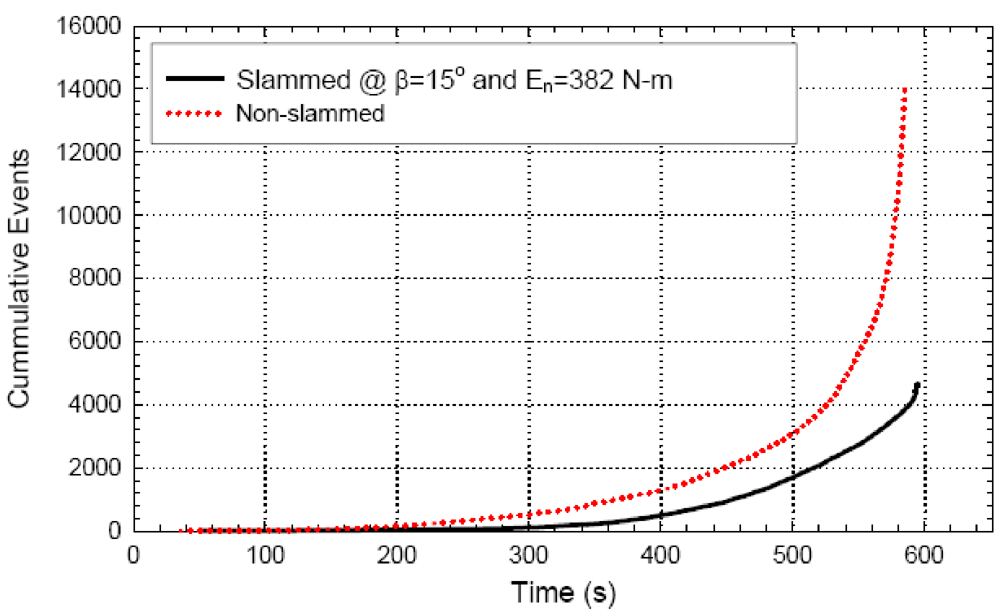

Figure 37: Cumulative acoustic emission activity of slammed and non-slammed samples

Acoustic emission (AE) can yield useful information regarding failure activity that may not be apparent with the strain sensors or strength reduction parameters. Figure 37 shows a comparison of cumulative AE activity obtained during the static flexural test for a typical slammed and non-slammed specimen. In spite of a general lack of flexural strength reduction observed in slammed specimens, a small but measurable reduction in the cumulative AE activity was consistently observed as illustrated for a typical case in Figure 37. This reduction in AE activity is substantially lower than what has been observed in other sandwich composite systems subjected to similar loading scenarios [52]. AE analysis, though indicating the presence of damage in the slammed specimens did not offer a clear trend as a function of deadrise angle β or slamming energy E_n, due perhaps to the large scatter observed.

7 DAMAGE ASSESSMENT OF FOAM CORE SANDWICH COMPOSITES UNDER REPEATED SLAMMING [59]

This chapter presents the results of repeated slamming of polyurethane foam core sandwich composites considering the effect of: deadrise angle (β) and slamming energy E_n.

7.1 Results and Discussion

A gradually decreasing lifetime was observed as a function of increasing slamming energy or decreasing deadrise angle, as seen in Fig. 38. E/E_n along the ordinate in these graphs represents the percentage of energy required for catastrophic failure under single slams. As most of the engineering design is based on conventional fatigue testing, an S-N curve was also generated for comparison with the E-N curve and is presented in Figure 38. This striking disparity however, appears logical as loads are localized, in continuous contact and gently applied quasi-statically in the case of fatigue and violent (truly dynamic) slamming event causing widespread damage in the case of repeated slamming. Under repeated slamming, none of the specimens failed at 45^o deadrise angle up to the 2000 cycle threshold under maximum slamming energy capacity of the machine. Fig. 38 also indicate an enormous scatter in the lifetime data with up to an order of magnitude difference in lifetimes under same testing conditions. Extensive scatter (although of somewhat smaller magnitude than currently observed) is typical in sandwich composites tested under fatigue, impact and even static loading conditions [32, 52, 54, 55]

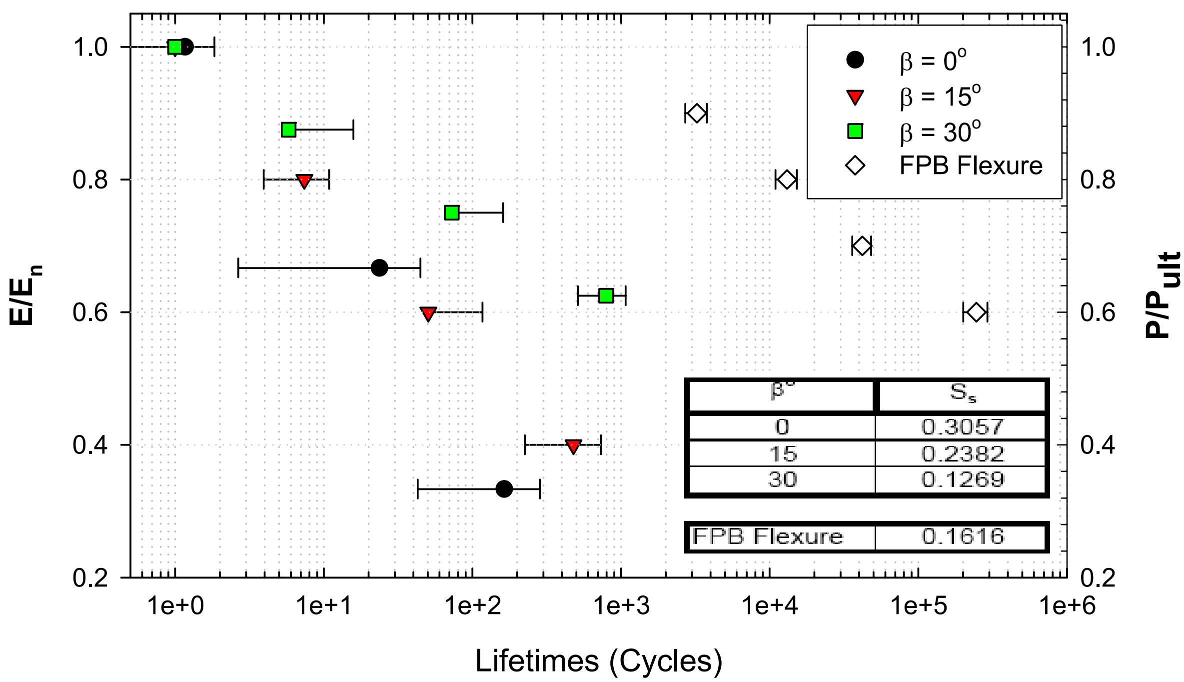

Figure 38: slamming energy ratio vs number of cycles to failure (E-N) data compared with conventional fatigue lifetime (S-N), error bars refer to the standard deviation

It is interesting to notice that the slopes of the slamming energy vs. lifetime (Fig. 38) decrease as the deadrise angle increases, indicating an increase in lifetime. Based on this experimental observation, a methodology is proposed to establish safe design and operational conditions.

Figure 39 shows the deadrise angles plotted against the E-N slopes. In the absence of slamming lifetime data at 45^o, it is not clear whether a linear or quadratic function would best describe the behavior, however, as none of the specimens failed at 45^o, a conservative quadratic relationship appears more likely. Based on Figure 39, the safe operational limit can be described as,

$$\frac{\beta}{\beta_e} + \left(\kappa \frac{S_s}{\varepsilon_u} \right)^2 = 1 \qquad (7)$$

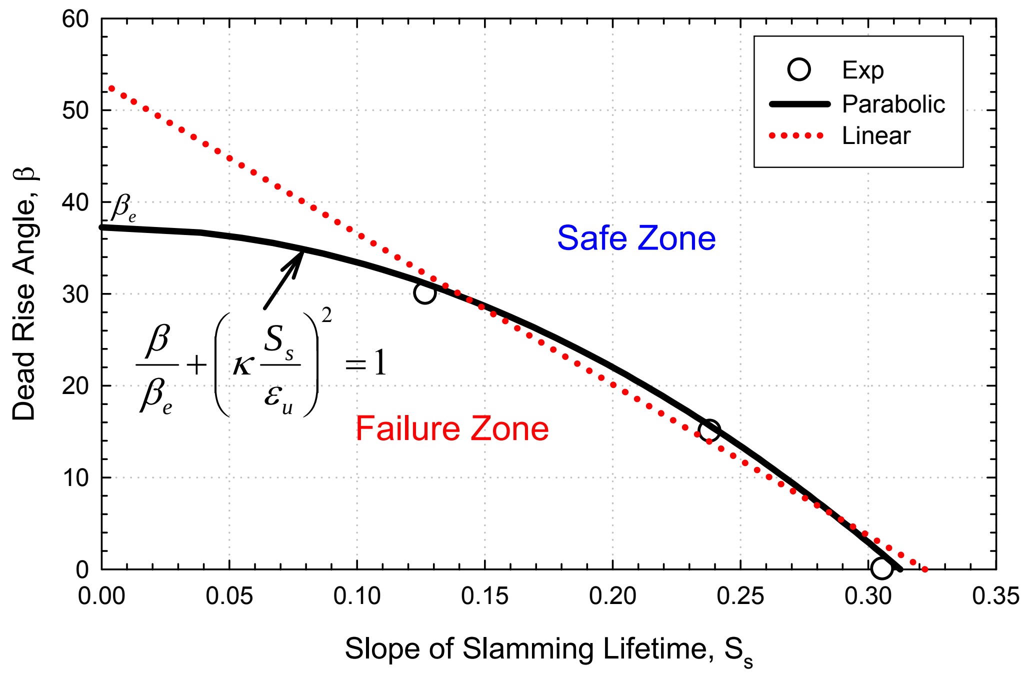

Figure 39: Proposed quadratic and linear operational safe limit, for repeated slamming

where β is the deadrise angle, β_e is the value along the ordinate of the quadratic function, κ is an experimentally adjusted parameter, ε_u represents the threshold strain causing catastrophic failure under single slam (~0.0035) and finally S_s is the slope of E/E_n vs N curve obtained from Figure 38. These observations are in accordance with the theoretical formulations present in the literature that indicate a gradual but significant reduction in peak pressures at higher deadrise angles [8, 12]; thus it is not surprising why failure is unlikely beyond a 30^o deadrise angle.

Detecting damage progression during repeated slamming is an illusive process. For example, cyclic strains yielded inconsistent and incoherent output due to highly discrete nature of strain data and associated difficulties in signal analysis. Similarly, discrete pressure outputs could not be used to extrapolate failure events. Acoustic emission sensors failed as they are not designed to record widespread damage and sustain highly violent and repetitive impacts. In the absence of viable real time damage detection instrumentation, various tests were interrupted at about 50% of the average repeated slamming life, the specimens were cut along the dashed lines indicated in Figure 5 and tested in flexural mode under static and fatigue loading to ascertain damage accumulated under repeated slamming. Contrary to reported results [52], there was disappointingly little evidence of accumulated damage when the slammed specimens were tested under static flexure as indicated in Figure 40. However, when the repeatedly slammed specimens were subjected to fatigue testing, a substantial reduction in life was observed as compared with non-slammed specimens (Figure 41). It is well established that fatigue tests offer more favorable conditions for damage progression in a material as opposed to static loading and the micromechanisms and modes of failure differ markedly under the two conditions [32]. After an exhaustive effort and for the current set of testing, it appears that post slamming fatigue is the only methodology that offers any measure of sustained damage under repeated slamming.

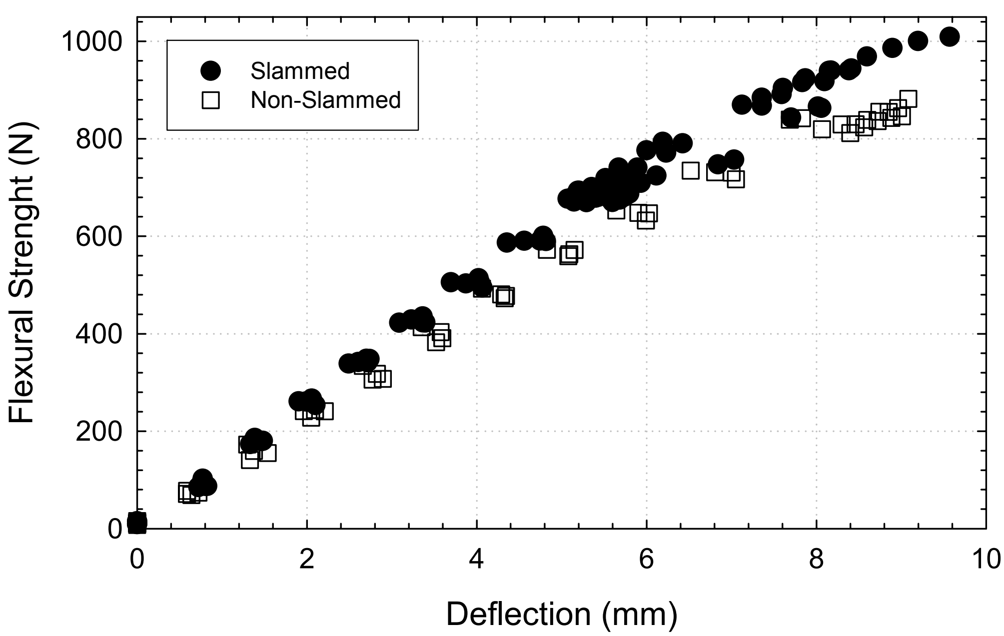

Figure 40: Flexural strength behavior under static test of slammed and non-slammed samples

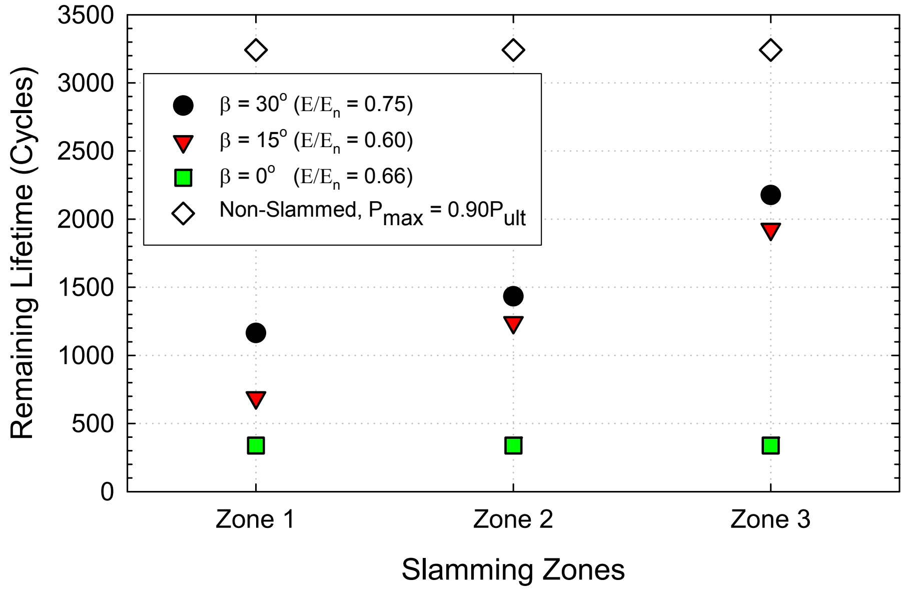

Figure 41: Zonal remaining fatigue lifetime of post slammed samples (50% of slamming lifetime)

Post slamming fatigue tests clearly indicate a reduction in life as a result of repeated slamming. However, the absence of any real time damage information poses a serious challenge in developing a quantitative damage assessment model. Based on the remaining lifetime from specimens interrupted at 50% of slamming lifetime and the slopes obtained in Figure 38 is proposed an methodology to assess damage induced by repeated slamming. The methodology assumes a conservative linear profile to assess damage progression during repeated slamming, with catastrophic failure corresponding to a damage coefficient of 1 as seen in Figure 42. The damage under slamming can then be written as

$$d_s(n) = \frac{n}{n_{sf}} \tag{8}$$

where d_s is the damage coefficient under slamming, n is slamming cycles, and n_{sf} is the life until catastrophic failure. Using the slopes obtained from Figure 38 at various deadrise angles and the post slamming fatigue life, a plot such as shown in Figure 42 for $\beta=0^0$ is generated. Notice that the post slamming fatigue curve shown in Figure 42 starts from the point when the damage accumulation begins, i.e., a change in shear modulus occurs. This plot can be described as

$$d_f(n) = \frac{e^{\alpha n c}}{e^{n_f c}} \tag{9}$$

where d_f is the damage coefficient under fatigue, C is an exponential coefficient obtained from changes in shear modulus, α value obtained from slamming lifetime slope, and n_f corresponds to the number of cycles to failure under fatigue. In order to obtain damage in terms of remaining fatigue life, a line corresponding to the desired slamming cycles is extended from slamming curve onto the fatigue life curve and the remaining life is shifted back to generate the actual life curves due to slamming and post slamming fatigue, as shown in Figure 43. Figure 43 also represents summation (Miner's rule) of slamming from Eq. 8 and fatigue from Eq. 9 to show total loss of life corresponding to various deadrise angles. It should be remembered that this methodology provides an alternative to the limitations imposed by the real time damage assessment instrumentation. Furthermore, the actual data presents enormous scatter which must be accounted for in making quantitative assessment.

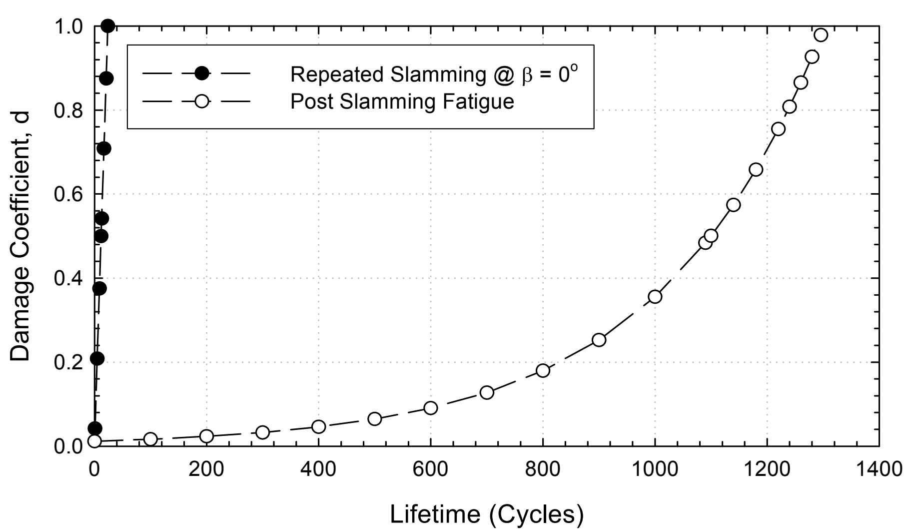

Figure 42: Damage coefficient evolution for repeated slamming and post slamming fatigue

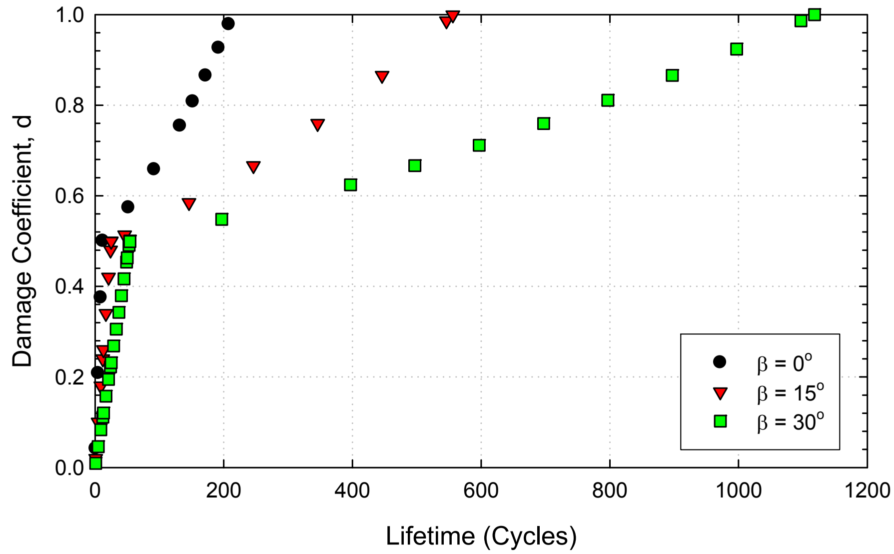

Figure 43: Two step damage representation under repeated slamming and post slammed fatigue results

The damage accumulation and onset of failure was observed to occur near the chine for 0° and 15° whereas the damage and failure shifted towards the keel at 30° and 45° angles. However, post slamming fatigue failure consistently occurred near the keel irrespective of the deadrise angle, thus clearly indicating greater accumulation of damage near the keel under repeated slamming. It should be noticed that peak pressures and strains were also always obtained near the keel irrespective of the deadrise angle, which agrees well with the literature [9, 12, 15]. Damage accumulation near the chine as opposed to the keel has been reported for honeycomb core sandwich composites that were tested at 20° angle[52]. Even though the reasons are not quite clear, the cause of such counter intuitive behavior appears to be embedded in the complex nature of wave propagation under slamming. To begin with, the amplitude of pressure pulse has been shown to reduce dramatically at deadrise angles beyond 30° and in fact the pressure does not peak at 45° angle [8]. This can cause a substantial change in the wave propagation mechanism and may explain the damage shift from the chine to the keel at higher angles.

From the elementary theory of wave propagation in rods, it is known that when a compression pulse is incident on a free boundary it gives rise to a reflected tension pulse.

Furthermore, the displacement of the end of the bar is twice its magnitude as the pulse traveling along the bar. The stresses produced by the incident and reflected pulses thus add up on the fixed boundary, and the values of the resultant stress are double the corresponding values when the pulse is traveling along the bar. Along the same lines, it may be argued that as the keel impacts the water, a shock wave propagates towards the chine edge, where it is immediately reflected as a tensile wave. So that immediately after reflection, the tensile stress (or momentum) gains twice the magnitude it had at the head of oncoming pulse. The reflected part of the pulse travels back to the source and is reflected again towards the chine. The interface of such reflected pulses may give rise to very complicated stress distributions and superposition of several reflected pulses appears to be responsible for the increased damage near the chine at lower deadrise angles. At higher deadrise angles, since the magnitude of pressure pulse is substantially muted, the wave propagation and reflection does not follow the same pattern. The complicated physical mechanisms that cause the shift in damage accumulation from keel to the chine as a function of deadrise angle are not completely understood. Particular difficulties are experienced in delineating slamming impulse, energy absorption and wave propagation and reflection which are responsible for such a behavior. However, it should be noted that the ship design is primarily based on peak pressure measurements that are always experienced near the keel under free drop conditions with the presumption that the critical damage must coincide with the same location as evidenced by several theoretical and experimental studies [4, 6, 8, 10, 11, 15, 23, 56].

Even though the dynamic slamming loads are almost uniformly distributed and the resulting damage is widespread, a single major damage site was observed under repeated slamming localized near the chine or the keel depending on the deadrise angle that lead to the catastrophic failure (see Figure 44). Under repeated slamming failure always occurred as a result of core tearing along the interface and subsequent core shear with some evidence of core densification; this phase consumed over 95% of the slamming life. Catastrophic failure manifested as facesheet separation caused by a rapid growth of core shear crack. Under slamming, there was little evidence to indicate any facesheet damage prior to catastrophic failure.

For post slamming fatigue specimens, modes of failure were predominantly core shear accompanied by local buckling of the facesheet on the compression side, indicating facesheets damage accumulation under slamming. The modes of failure under fatigue of non-slammed specimens point exclusively to core shear with no evidence of facesheet buckling. Even though the specimens cut near the keel showed a marked reduction in fatigue life as compared to the chine, the modes of failure near the keel or the chine were nearly identical.

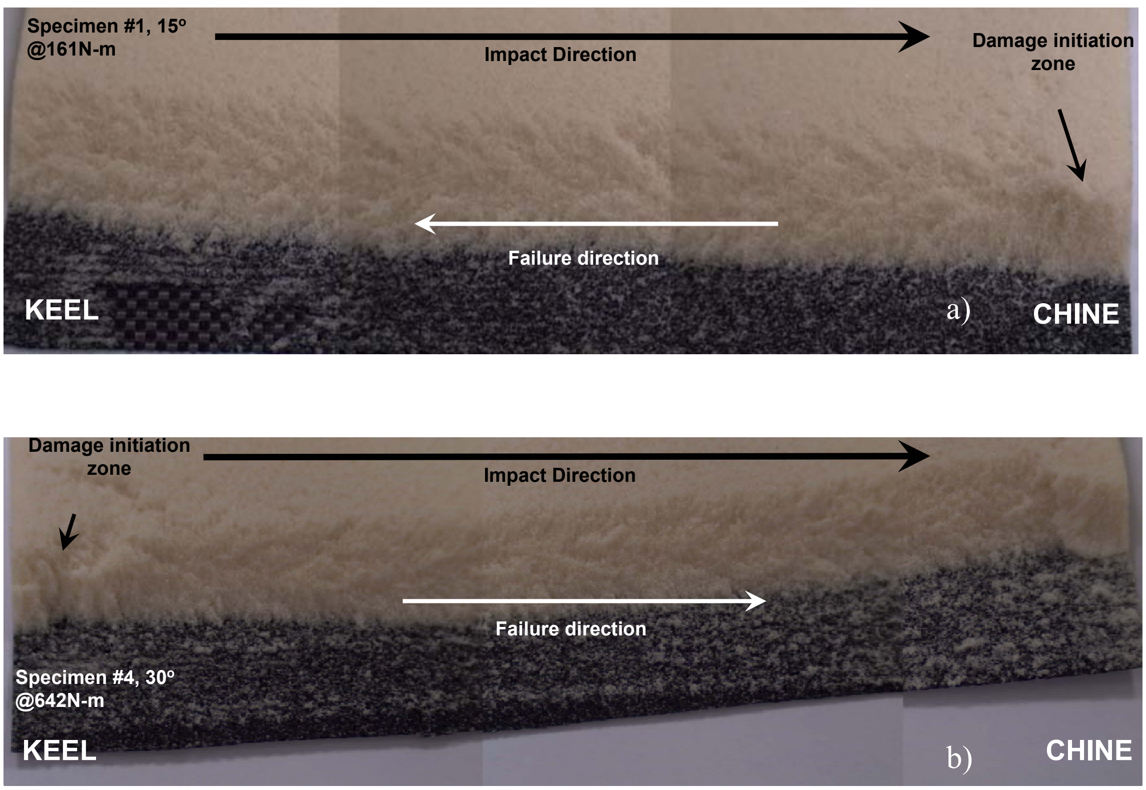

Figure 44: Typical failure pattern at a) $\beta = 15^o$ and b) $\beta = 30^o$

8 CONCLUSIONS

1. *Fatigue:* Acoustic emission analysis yielded very accurate information about the extent and location of damage in various constituents of sandwich composites. AE and post-test analysis indicated core shear to be the predominant damage mechanism followed by interfacial failure, whereas fiber rupture triggered the onset of catastrophic failure. A large scatter in the data was observed a characteristic feature of a multi-constituent material like sandwich composite.

2. *Slamming of Honeycomb Core Sandwich Composites:* Acoustic emission based post slamming damage assessment on single and repeated slammed honeycomb sandwich composite panel revealed otherwise hidden cumulative damage. In single slam tests, damage was found to be highest near the chine while pressure and strain consistently peaked near the keel; this trend, however, was not seen under repeated slamming. Repeated slamming showed widespread damage in the material. For both single and multiple slammed specimens, substantial damage was found even at a very low slamming energy that left no visible/apparent damage in the specimen.

3. *Single Slamming of Foam Core Sandwich Composites:* An increase in the probability of failure was observed as a function of increasing slamming energy (E_n) or decreasing deadrise angle (β). Slamming pressure is a useful design parameter; however, it provides limited information on the failure/damage processes of the material. Although strain data was discrete, it offered useful insight regarding the state of damage in the composite material. Theoretical formulation based on quasi-static analysis was successfully employed to assess peak strains during slamming by introducing a hydroelasticity function. Due to the highly brittle nature of the material, there was very little loss in flexural capacity of the foam core sandwich composite panel under non-catastrophic slamming. This result was corroborated by the microscopic and AE analysis.

Modes of failure were primarily core shear along the interface, local facesheet buckling and resin fragmentation under slamming.

4. *Repeated Slamming of Foam Core Sandwich Composites:* Repeated slamming on foam core sandwich composite materials indicated an increase in life as a function of increasing deadrise angle or decreasing slamming energy. Using the slopes of E-N curves, a methodology is suggested for safe operational and design conditions. Furthermore, an indirect methodology in terms of remaining fatigue life is proposed in order to account for the damage accumulation under repeated slamming. In-spite of widespread damage, failure was localized to a single site near the chine or the keel depending on the deadrise angle. Failure modes primarily corresponded to core tearing along the interface and core shear in the case of repeated slamming with little evidence of facesheet damage prior to catastrophic failure, whereas, post slamming fatigue indicated core shear accompanied by local facesheet buckling.

9 FUTURE WORK

- Damage assessment under repeated slamming must be improved by probing deeper into the damage accumulation mechanisms. The assumed linearity in damage evolution in repeated slamming must be verified experimentally by designing innovative tests and instrumentation to monitor cyclic damage. The many problems, such as, discreteness, recalibration, short circuiting, etc. associated with strain gages that have been the main source of damage information must be somehow overcome in order to obtain meaningful data.

- Repeated slamming is crucial for proper design and safe life operations, however, the tests are quite time consuming and cumbersome. This may be overcome by automating the test setup and integrating the testing apparatus with some neural network type of software that can provide real time damage information.

- Testing needs to be extended to various sandwich composite material systems, such as balsa core and different types of cores. The effect of density and thickness of the core is another crucial parameter that effects the slamming lifetime and needs to be considered.

- As the marine applications extend to military operations of the ships, slamming of post ballistic impact of ships can provide essential clues as to the survivability under more critical conditions.

- A purely analytical model is not expected until cyclic damage progression is properly understood. However, semi-empirical models based on FEA can form a basis of long term damage assessment.

10 REFERENCES

1. Rosén, A., Garme, K., (2004). Model Experiment Addressing The Impact Pressure Distribution on Planning Craft in Waves, *International Journal of Small Craft Technology,* 146:11-20.

2. Garme, K., Rosén, A., (2003). Time-Domain Simulation and Full Scale Trials on Planning Craft in Waves, *International Shipbuilding Progress*, 50(3):177-208.

3. Rosén, A. (2005). Impact pressure distribution reconstruction from discreet point measurements, *International Shipbuilding Progress*, 52(1):91-107.

4. Rosen, A. (2004). Loads and Responses for Planning Craft in Waves, *KTH Division of Naval Systems*, ISBN 91-7283-936-8.

5. Engle, A. and Lewis, R. (2003). A Comparison of Hydrodynamic Impacts Prediction Methods With Two Dimensional Drop Test Data, *Marine Structures*, 16:175-182.

6. Downs, R., Edinger, S., Battley, M. (2006). Slam Testing of Sandwich Panels, *SAMPE Journal*, 42(4):47-55.

7. Tayman, B., Haug, T. and Valsgard, S. (1992). Slamming Drop Tests on a GRP Sandwich Beams Subjected to Slamming Loads, *EMAS, Sandwich Constructions 2*:583-604.

8. Faltinsen, O. (2005). Hydrodynamics of High-Speed Marine Vehicles, *Cambridge University Press*, New York, New York.

9. Wagner, H. (1932). Uber stoss und gleitvergange an der oberflache von flossigkeiten, *Z. Ang. Math. Mech,* 12:192-253.

10. Karman, V. (1929). The Impact on the Seaplane Floats During Landing, *Technical Notes*, Vol. TN 321:1-8.

11. Breder, J. (2005). Experimental Testing of Slamming Pressure on a Rigid Marine Panel, *KTH (Sweden) Center for Naval Architecture*, Master's Thesis.

12. Zhao, R., Faltinsen, O. (1993). Water Entry of Two-Dimensional Bodies, *Journal of Fluid Mechanics*, 246:593-612.

13. Bereznitski, A. (2005) "Slamming: The role of hydroelasticity", *International Shipbuilding Progress*, 48(4):333-351.

14. Campana, E., Carcaterra, A., Ciappi, E. and Iafrati, A. (2000) Some Insights Into Slamming Forces: Compressible and Incompressible Phases, *Proceedings of Institution of Mechanical Engineers (*IMechE), 214(Part C):881-888.

15. Stenius, I. (2006). Finite Element Modeling Of Hydroelasticity in Hull-Water Impacts, *KTH (Sweden) Center for Naval Architecture*, ISBN: 978-91-7178-548-0.

16. Bereznitski, A., Kaminski, M.L., (May 2002), Practical Implications of Hydroelasticity in Ship Design. *Proceedings of the 12th International Offshore and Polar Engineering Conference*. Kitakyushu, Japan: 486-491.

17. Faltinsen, O.M., (1997) The Effect of Hydroelasticity on Ship Slamming. *Phil. Trans. R. Soc. London A*, 355:575-591.

18. Carcaterra, A., Ciappi E., (2003) Hydroynamic Shock of the Elastic Structure Impacting on the Water: Theory and Experiments. *Journal of Sound and Vibration,* 271:411- 439.

19. Tveitnes, T., (2001), Application of Added Mass Theory in Planing, *Thesis 12640 University of Glasgow*, Scotland, U.K.

20. Battley, M., Stenius, I., Breder, J., Edinger, S. (2005). Dynamic Characterization of Marine Sandwich Structures, Sandwich Structures 7: *Advancing with Sandwich Structures and Materials*, Springer, 537-546.

21. Wraith, R. (1998). Pressure Loads on Ship Hull Plating Caused By Slamming, Thesis, *Department of Mechanical and Manufacturing Engineering, The University of Melbourne, Australia.*

22. Yettou, E., Desrochers, A. and Champoux, Y. (2007), A New Analytical Model for Pressure Estimation of Symmetrical Water Impact of a Rigid Wedge at Variable Velocities, *Journal of Fluids and Structures*, 23(3):501-522.

23. Davis, R.D., Whelan, J.R., (2006), *Modeling Wet Deck Bow Slamming of Wave Piercing Catamarans.* International Journal of Maritime Engineering, A3: 42-57.

24. Kvalsvold, J., Faltinsen, O., (1995), *Hydroelastic Modeling of Wet Deck Slamming on Multihull Vessels.* Journal of Ship Research, 39:225-239.

25. Buene, L., Echtermeyer, A., Sund, O., Nydgard, M. and Hayman, B. (1991). Assessment of Long Term Effects of Slamming Loads on FRP Sandwich Panels, *International Conference on Fast Sea Transportation,*1:365-380.

26. Burman, M., (2000) *Fatigue Crack Initiation and Propagation in Sandwich Structures.* Doctoral Thesis Report 98-29, Royal Institute of Technology.

27. Mahi, A., Farooq, M., and Sahraoui, D., (2002) “Mechanical behavior of Sandwich Composite Material under Cyclic Fatigue”, *New Trends in Fracture and Fatigue,* April, Metz France.

28. Kulkarni N, Mahfuz H., Jeelani H., and Carlsson L.A., (2005), *Fatigue Crack Growth and Life Prediction of Foam Core Sandwich Composite under Flexural Loading.* Composite Structures, 59:499-505.

29. Avery J.L., (2000), *Compressive Failure of Sandwich Beams with Debonded Face Sheets.* Journal of Composite Materials, 34(14):1177-1199.

30. Caprino G., (2000), *Predicting Fatigue Life of Composite Laminates Subjected to Tension-Tension Fatigue.* Journal of Composite Materials, 34(16):1334-1355.

31. Kazimierz, S., Spencer, B.F., (1992), *Random Fatigue: From Data to Theory*, *Academic Press*: New York, ISBN 0126542252.

32. Sharma, N., Gibson, R., Ayorinde, E., (2006) "Fatigue of foam and honeycomb core composite sandwich structures: A tutorial", Journal of Sandwich Structures and Materials, 8:263-319.

33. Bakukas, J.K., Proser, W.H. and Jonhsont, W.S., (1994) *Monitoring Damage Growth in Titanium Matrix Composites Using Acoustic Emission.* Journal of Composite Material, 28(4):305-328.

34. Daniel, I.M, (1999), *Experimentation and Modeling of Composite Materials.* Experimental Mechanics, 39(1):1-19.

35. Harris, D. and Dunegan, H., (1974)"Continuous Monitoring of Fatigue Crack Growth by Acoustic Emission Technique", *Third SESA International Congress on Experimental Mechanics*, Los Angeles California.

36. Vargas, A., (1985) "Acoustic Emission for Quality Control in Composites", *Physical Acoustic Corporation*, Princeton Junction, TR-103-58-6/85, New Jersey.

37. Li, F., and Li Z., (2000), Acoustic Emission Monitoring of Fracture of Fiber-Reinforced Concrete in Tension. *ACI Materials Journal,* 97(6):629-636.

38. Prosser, W., (1995), Advanced Waveform-Based Acoustic Emission Detection of Matrix Cracking in Composites. *Materials Evaluation,* 53:1052-1058.

39. Nondestructive Testing Handbook, 2nd ed. (1987), *American Society for Nondestructive Testing* 5, ASNT, New Jersey.

40. Huang, M., (1998), Using Acoustic Emission in Fatigue and Fracture Materials Research. *JOM*, 50(11):1-14.

41. English, L., Listen and Learn, (1987), AE Testing Composites. *Physical Acoustic Corporation,* TR103-75-6/87, 1987, New Jersey.

42. Quispitupa, A., Shafiq, B., Just, F., Serrano, D., (2004), *Acoustic Emission Based Tensile Characteristics of Sandwich Composites.* Composites Part B: Engineering, 35 (6-8):563-571.

43. Vaidya, U., Abraham, A., and Bhide, S., (2001), Affordable processing of thick section and integral multi-functional composites. *Composites Part A*, 32(8):1133-1142.

44. ASTM, *Standard Guide for Determining the Reproducibility of Acoustic Emission Sensor Response1.* ASTM, 2000. E 976.

45. Sharma, S., Krishna, M., Murthy, H., Battacharya, D., (2004), Fatigue studies of polyurethane sandwich structures, *Journal of Materials Engineering and Performance*, 13 (5):637-641.

46. Zenkert, D. (1997), Handbook of Sandwich Construction, *Engineering Materials Advisory Services, Ltd.*

47. Sharma, N., Gibson, R., Ayorinde, E., (2006), Fatigue of foam and honeycomb core composite sandwich structures: A tutorial, *Journal of Sandwich Structures and Materials*, 8:263-319.

48. Sutherland, L., Soares, G., (2006), *Impact behavior of typical marine composite laminates.* Composites: Part B, 37:89-100.

49. Yettou, E., Desrochers, A. and Champoux, Y. (2007). A New Analytical Model for Pressure Estimation of Symmetrical Water Impact of a Rigid Wedge at Variable Velocities, *Journal of Fluids and Structures*, 23(3):501-522.

50. Hayman, B., Haug, T., Valsgard, S., (1991), S., H.B.H.T.a.V., *Response of Fast Craft Hull Structures to Slamming Loads.* International Conference of Fast sea Transportation, 1:381-388.

51. Thomas, G., Davis, M., Holloway, D., Watson, N., and Roberts, T., (2003), *Slamming Response of a large high-Speed Wave-Piercer Catamaran.* Maritime Thechnology, 40 (2):126-140.

52. Charca S., Shafiq, B., and Just F., (2008), *Repeated Slamming of Sandwich Compositeson Water* Acepted to Journal of Sandwich Structures and Materials, December 2008.

53. Shenoi, R.A., Wellicome, J.F., (1993) *Composites Materials in Maritime Structures*. Ocean Technology, ed. Cambridge. Vol. 2.

54. Shafiq, B., Quispitupa, A., (2005), *Fatigue Characteristics of Foam Core Sandwich Composites.* International Journal of Fatigue, 28(2):96-102.

55. Bartus, S.D, (2007) *A review: impact damage of composite materials.* Journal of Advanced Materials, 39(3):3-21.

56. Yettou, E., Desrochers, A. and Champoux, Y. (2006.) Experimental Study on the Water Impact of a Symmetrical Wedge, *Fluid Dynamics Research*, 38(1):47-66.

57 Charca, S., Shafiq, B., Gonzalez, S., Lopez, O., Just, F., (March 2009), Fatigue Life Assessment of Foam Core Sandwich Composites, submitted to *Journal of Advance Materials (JAM)*.

58 Charca, S., Shafiq, B., (December 2008), Damage Assessment Due to Single Slamming of Foam Core Sandwich Composites, accepted to *Journal of Sandwich Structures and Materials*.

59 Charca, S., Shafiq, B., (March 2009), Damage Assessment Due to Repeated Slamming of Foam Core Sandwich Composites, submitted to *Journal of Sandwich Structures and Materials*.

60 Clark, S.D, Shenoi, R.A., Allen H.G., (1999), "Modelling the fatigue behaviour of sandwich beams under monotonic, 2-step and block-loading regimes", *Composites Science and Technology*, 59:471-486.

APPENDIX A: SHEAR MODULUS

Notation:

n Slamming and fatigue lifetime

n_{if} Number of Cycles to damage initiation

N_f Number of cycles to catastrophic failure

$n_f = N_f - n_{if}$ Total number of cycle after damage initiated

Deflection for simply supported beam is the sum of the static and fatigue shear components, and for four point bend (FPB) loading the deflection at the loading point can be expressed as:

$$\delta_T\left(n/N_f\right) = \delta_b + \delta_s\left(n/N_f\right) \tag{A1}$$

Where

$$\delta_b = \frac{PL^3}{56D} \tag{A2}$$

$$\delta_s\left(n/N_f\right) = \frac{PL}{6AG_f(n/N_f)} \tag{A3}$$

here P is the total load applied, A is the cross section area and L is the span length; the term n/N_f is a normalized fatigue lifetime with respect to failure lifetime. The experimental shear deflection and shear modulus can be calculated directly from the total deflection, as the static bending deflection is independent of the number of cycles, the corresponding term remains constant along the entire fatigue lifetime. Using the model suggested by Clark et al [60], the shear modulus along the fatigue lifetime is expressed as:

$$G_f(n) = G_o; \qquad n \le n_{if} \tag{A4}$$

$$G_f\left(n/N_f\right) = G_o - Ae^{(\frac{n}{N_f})C}; \qquad n \ge n_{if} \tag{A5}$$

where the parameters A and C are obtained experimentally by simple curve fitting

APPENDIX B: DAMAGE MODEL

Considering two steps loading condition and using the linear Miner's rule the damage is:

$$1 = d_s + d_f \tag{B1}$$

where d_s and d_f are the fraction of damage induced by the slamming loading and conventional fatigue loading. Damage progression based on the shear modulus degradation can then be defined as:

$$D_f\left((n - n_{if})/n_f\right) = \frac{G_o - G_f\left((n - n_{if})/n_f\right)}{G_o - G_f\left(n_f / n_f\right)} \quad n \geq n_{if} \tag{B2}$$